

Manganese(III) Nitrate Complexes as Bench-Stable Powerful Oxidants

Ananya Saju, Dr. Matthew R. Crawley,[†] Dr. Samantha N. MacMillan,[§] Prof. David C. Lacy^{*†}

[†]Department of Chemistry, University at Buffalo, State University of New York, Buffalo, New York 14260, United States.

[§]Department of Chemistry and Chemical Biology, Cornell University, Ithaca, New York 14853, United States.

Index

Contents	Page
Experimental methods: general considerations	2
Crystallographic methods	2
Synthesis and characterization of manganese(III) complexes	2
<i>Synthesis and characterization of [Mn(NO₃)₃(OPPh₃)₂] (2)</i>	2
<i>Synthesis and characterization of [Mn(NO₃)₃(OAsPh₃)₂] (4)</i>	5
<i>Synthesis and characterization of [Mn(NO₃)(MeCN)(Opy)₄][Mn(NO₃)₄] (5)</i>	6
<i>Synthesis and characterization of [MnCl₂(NO₃)(OPPh₃)₂] (6)</i>	8
<i>Synthesis and characterization of [MnCl₃(OAsPh₃)₂] (7)</i>	10
<i>Synthesis and characterization of [MnCl₂(NO₃)(OAsPh₃)₂] (8)</i>	11
<i>Characterization of [Mn(NO₃)₂(OPPh₃)₂] (9)</i>	13
EPR spectra of selected complexes	13
Determining solubility of 2 in fluorobenzene	14
Electrochemistry Experiments	14
Single-electron oxidation reactions	23
<i>Oxidation of ferrocene by 2</i>	23
<i>Oxidation of [Fe(bipy)₃](PF₆)₂ by 2</i>	23
<i>Oxidation of tris(4-bromophenyl)amine by 2</i>	24
General procedure for solvent screen for HMB nitroxylation	25
General procedure for nitroxylation reactions	25
References	28

Experimental methods: general considerations

All chemicals were purchased from chemical vendors and used as received unless otherwise noted. Dry, oxygen-free solvents were obtained from a PPT solvent purification system and were stored over 3 Å molecular sieves prior to use. ACS grade fluorobenzene was degassed by 4 freeze-pump-thaw cycles, stored under 3 Å molecular sieves for 24h, and further dried by passing through a plug of dried basic alumina before use. Unless otherwise stated, all manipulations were performed in a nitrogen filled VAC glovebox or on a Schlenk line. NMR experiments were carried out on Bruker Neo-400 MHz or Bruker Neo-500 MHz spectrometers. EPR experiments were carried out on EMX 390 EPR Spectrometer. ATR-FTIR spectra were collected using a Bruker Alpha IR spectrometer with the “ATR Platinum” insert adapter (diamond crystal) stored inside a nitrogen filled VAC Atmospheres glovebox. Voltammetry experiments were performed using a SP-200 Bio-Logic potentiostat. UV-vis experiments were performed using an 8154 Agilent Spectrophotometer equipped with an Unisoku cryostat. CHN combustion analyses were performed using a Thermo Scientific FlashEA1112 CHNS analyzer. The following compounds were prepared according to literature: $[\text{Mn}_{12}\text{O}_{12}(\text{OAc})_{16}(\text{H}_2\text{O})_4] \cdot 2\text{HOAc} \cdot 4\text{H}_2\text{O}$ (**Mn₁₂**),¹ $[\text{Fe}(\text{bipy})_3](\text{PF}_6)_2$,² $[\text{MnCl}_3(\text{OPPh}_3)_2]$ (**1**),³ and *tert*-butyldiphenyl(*p*-tolylxy)silane.⁴

Crystallographic methods

Low-temperature X-ray diffraction data for $[\text{Mn}(\text{NO}_3)_3(\text{OPPh}_3)_2]$ (**2**), $[\text{Mn}(\text{NO}_3)_3(\text{OAsPh}_3)_2]$ (**4**), $[\text{Mn}(\text{OPy})_4(\text{MeCN})(\text{NO}_3)]$ $[\text{Mn}(\text{NO}_3)_4]$ (**5**), $[\text{MnCl}_2(\text{NO}_3)(\text{OPPh}_3)_2]$ (**6**), $[\text{MnCl}_3(\text{OAsPh}_3)_2]$ (**7**), and $[\text{MnCl}_2(\text{NO}_3)(\text{OAsPh}_3)_2]$ (**8**), and $[\text{Mn}(\text{NO}_3)_2(\text{OPPh}_3)_2]$ (**9**) were collected on a Rigaku XtaLAB Synergy diffractometer coupled to a Rigaku Hypix detector with either Cu K α radiation ($\lambda = 1.54184$ Å) or Ag K α radiation ($\lambda = 0.56087$ Å, for **8**), from PhotonJet micro-focus X-ray sources at 100 K (293 K for **2**). The diffraction images were processed and scaled using the CrysAlisPro software.⁵ The structures were solved through intrinsic phasing using SHELXT⁶ and refined against F² on all data by full-matrix least squares with SHELXL⁷ following established refinement strategies.⁸ All non-hydrogen atoms were refined anisotropically. All hydrogen atoms bound to carbon were included in the model at geometrically calculated positions and refined using a riding model. The isotropic displacement parameters of all hydrogen atoms were fixed to 1.2 times the U_{eq} value of the atoms they are linked to. **7** was refined as a two-component non-merohedral twin, BASF 0.3254(8). A Mn(II) bis(nitrato) complex co-crystallized with **6** and was modeled with 9.9(2)% occupancy. Analogous to **6**, complex **8** exhibited 12.0(3)% occupancy co-crystallized **7** and the Mn-center was positionally disordered so that the $\text{MnCl}_2(\text{NO}_3)$ and MnCl_3 units comprised the two-part disorder model. The stated occupancies for **6** and **8** were refined using a single free variable.

Synthesis and characterization of manganese(III) complexes

Synthesis and characterization of $[\text{Mn}(\text{NO}_3)_3(\text{OPPh}_3)_2]$ (**2**)

One-pot synthesis (in glovebox): In a 50 mL round bottom flask equipped with a stir bar, AgNO_3 (6.88 g, 40.5 mmol, 16 eq.) was dissolved in 25 mL MeCN and Me_3SiCl (5.09 mL, 40.5 mmol, 16 eq.) was added dropwise under constant stirring for 15 minutes to generate $\text{Me}_3\text{SiONO}_2$ *in-situ*. KMnO_4 (0.400 g, 2.53 mmol, 1.0 eq.) and $\text{Mn}(\text{OAc})_2$ (1.75 g, 10.1 mmol, 4.0 eq.) were stirred in 35 mL MeCN in a 250 mL round bottom flask. The $\text{Me}_3\text{SiONO}_2$ solution was filtered (15 mL glass frit with celite) directly into the second mixture to give brown solution **3**; 10 mL of MeCN was used to wash any remaining $\text{Me}_3\text{SiONO}_2$ into the reaction flask through the frit. Ph_3PO (5.64 g, 20.3 mmol, 8.0 eq.) was added to the reaction mixture after 15 minutes of stirring at room temperature. The reaction mixture was allowed to stir for 1.5 hours during which a brown precipitate form. The precipitate was filtered out and washed with minimal amount of MeCN and Et_2O then dried under vacuum. This solid was dissolved in DCM, the saturated solution filtered over a small celite plug, and layered under pentane at room temperature to yield crystals of **2** which were washed with pentane and dried under vacuum to yield crystalline **2** (5.08 g, 63%).

15 g scale synthesis: Following the procedure for one-pot synthesis in glovebox with 12.9 g AgNO_3 , 8.25 mL Me_3SiCl , 750mg KMnO_4 , 3.285 g $\text{Mn}(\text{OAc})_2$, and 10.7 g Ph_3PO in a total volume of 130 mL MeCN furnished 8.31 g of **2** (55%, crude) in 3.5 hours.

One-pot synthesis (on Schlenk line): This procedure was performed on a Schlenk line under argon at room temperature without maintaining rigorous air free conditions. The glassware was not oven dried. Solvent from PPT solvent purification system was dispensed into measuring cylinder open to air. The reaction mixtures were blanketed with argon during the reaction and both filtration steps were performed open to air with an inverted funnel attached to a Schlenk line above it to direct a gentle flow of argon onto the filtration apparatus.

In a 100 mL Schlenk flask equipped with a stir bar, AgNO_3 (4.30 g, 25.3 mmol, 16 eq.) was dissolved in 15 mL MeCN. Under a flow of argon, Me_3SiCl (3.13 mL, 25.3 mmol, 16 eq.) was added dropwise using a syringe under constant stirring, and stirred for 15 minutes, to generate $\text{Me}_3\text{SiONO}_2$ *in-situ*. In separate 100 mL Schlenk flask, KMnO_4 (0.250 g, 1.58 mmol, 1.0 eq.) and anhydrous $\text{Mn}(\text{OAc})_2$ (1.10 g, 6.33 mmol, 4.0 eq.) were stirred in 25 mL MeCN under argon. The *in-situ* prepared $\text{Me}_3\text{SiONO}_2$ solution was filtered (30 mL glass frit with celite) and added to the Mn-containing solution to give brown solution **3**. 10 mL of MeCN was used to wash any remaining

Me₃SiONO₂ into the reaction flask. After 15 minutes of stirring, Ph₃PO (3.52 g, 12.7 mmol, 8.0 eq.) was added as a solid to the reaction mixture and this was allowed to stir for 2 hours. The resulting brown precipitate was isolated by vacuum filtration and then washed with Et₂O (10 mL x 3) to afford 2.97 g of crude product (59%). The crude compound was dissolved in DCM, the saturated solution filtered over a small celite plug, and then layered under pentane at room temperature to yield crystals of **2**. The crystals were separated by open-to-air filtration and washed with minimal volume of MeCN to remove trace amount of a brown oil deposited on the crystals, followed by Et₂O, and then dried under vacuum to obtain crystalline **2** (772 mg, 26%). Note: if the crystallization was carried out under air-free conditions, the crystalline yield is increased to 51%.

From Mn₁₂: In a 20 mL scintillation vial equipped with a stir bar, AgNO₃ (149 mg, 0.877 mmol, 36 eq.) was dissolved in 2 mL MeCN and Me₃SiCl (0.110 mL, 0.876 mmol, 36 eq.) was added dropwise under constant stirring to generate Me₃SiONO₂ *in-situ*. Mn₁₂ (50.0 mg, 0.0243 mmol, 1.0 eq.) was stirred in 3 mL MeCN in another 20 mL scintillation vial to give an intense coffee brown solution. The Me₃SiONO₂ was filtered through celite and added into this reaction mixture to form a deep brown solution which was allowed to stir for 15 minutes before the addition of Ph₃PO (162 mg, 0.582 mmol, 24 eq.). 1 mL of MeCN was used to wash any remaining Me₃SiONO₂ into the reaction flask through the frit. The reaction mixture was allowed to stir at room temperature for 1 hour. The reaction mixture was then filtered and all volatiles were removed under vacuum to obtain a red-brown oil. The oil was dissolved in 3 mL DCM, the saturated solution filtered over a celite plug, and layered under pentane at room temperature to yield crystals of **2**. The crystals were washed with pentane and dried under vacuum to yield crystalline **2** (61.1 mg, 26%).

ATR-FTIR (cm⁻¹): 3056, 1552, 1524, 1436, 1304, 1260, 1149, 1118, 1063, 993, 967, 954, 797, 754, 723, 688, 531, 478, 434, 412.

¹H-NMR (CD₃CN): 8.22, 7.40.

Evans' method (dichloromethane-*d*₂, 500 MHz, 298 K) μ_{eff} = 5.46 μB.

CHN [Calc. (found)] for (C₃₆H₃MnN₃O₁₁P₂)•0.35CH₂Cl₂: % C 52.78 (53.04), % H 3.74 (3.79), % N 5.08 (4.76).

UV-vis ; solvent, λ_{max} [nm (ε, M⁻¹cm⁻¹): MeCN, 335 (1300), 500 (160); DCM, 315 (2500), 474 (240).

NOTE: Purity of recrystallized **2** was confirmed by performing nitroxylation of hexamethylbenzene (HMB) following general procedure for nitroxylation reactions. **2** is considered to be of good purity if near quantitative conversion of HMB to 2,3,4,5,6-pentamethylbenzyl nitrate is achieved.

Comments on solvent stability of **2**: Stability of solutions of **2** varies depending on the solvent.

DCM: saturated solutions of **2** in DCM (obtained from PPT solvent purification system) is stable indefinitely at room temperature in the glovebox or up to 2 days exposed to air. If ACS grade DCM is used without drying over sieves, the solution decomposes gradually over few hours to give a brown precipitate.

MeCN: solutions of **2** in MeCN behave similarly to those in DCM except within the context of MeCN being more susceptible to accumulating water. Solutions of **2** in MeCN open to air decompose within a few hours.

THF: solutions of **2** in dry THF (obtained from a PPT solvent purification system) steadily decomposes over ≈3 hours at room temperature in the glovebox. Furthermore, MeCN or DCM solutions of **2** in contact with THF or Et₂O decolorize within 24 h.

Fluorobenzene: solutions of **2** in dry fluorobenzene (degassed by 4 freeze-pump-thaw cycles, stored under 3 Å molecular sieves for 24h) decomposes under 30 minutes at room temperature in the glovebox. However, solution of **2** is stable for ~10 hours in the glovebox if the solvent is further dried by passing through dried basic alumina. The decomposition in most solvents appears to be through contact with water.

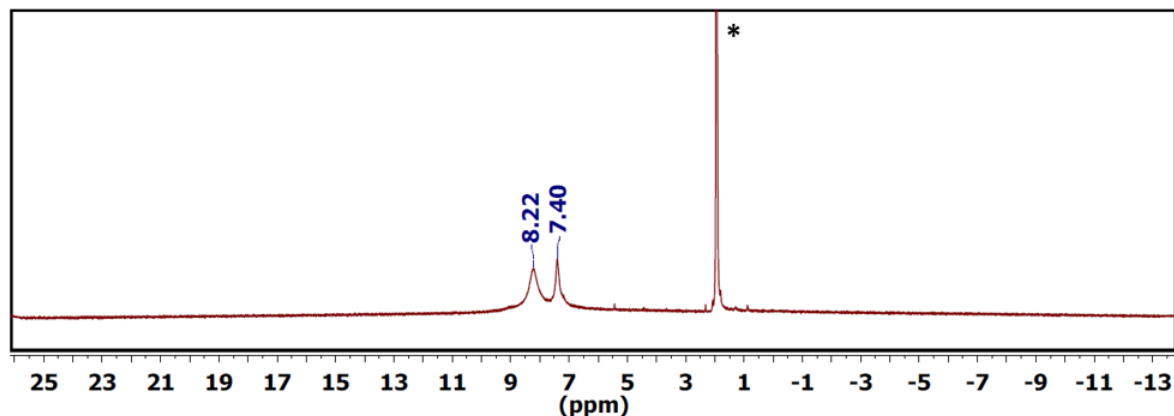


Figure S1: ¹H-NMR spectrum of **2** in CD₃CN(*).

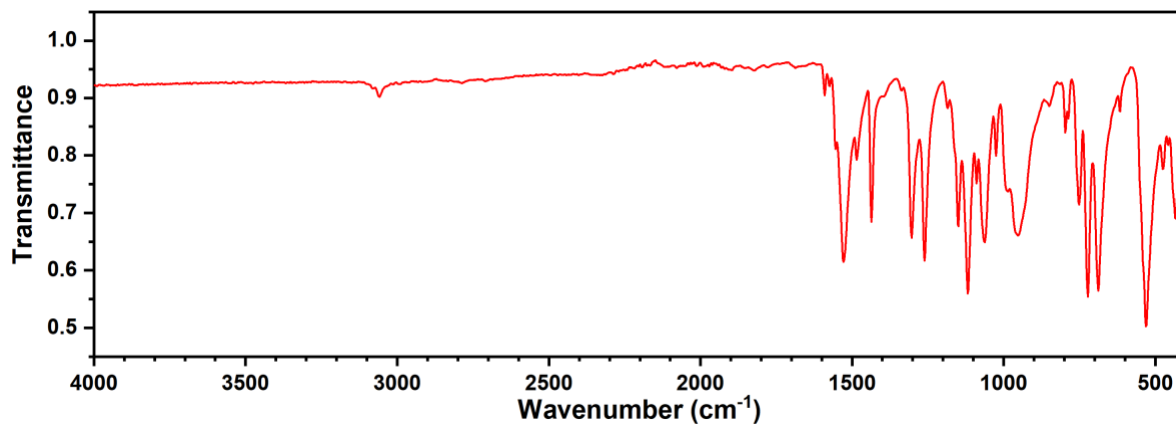


Figure S2: ATR-FTIR spectrum of **2**.

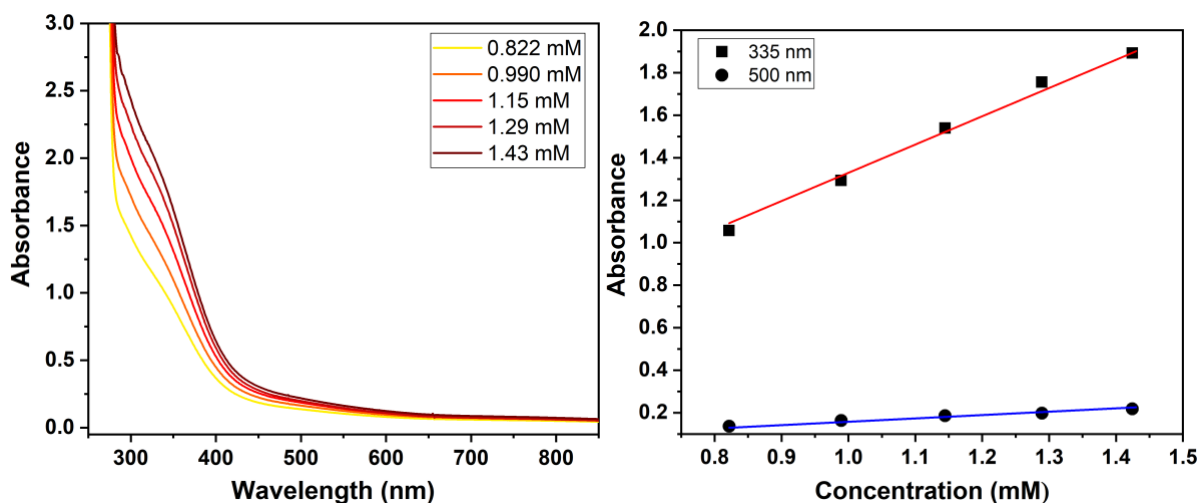


Figure S3: UV-vis spectra of **2** in MeCN at various concentration (left) with corresponding Beer's law plot (right).

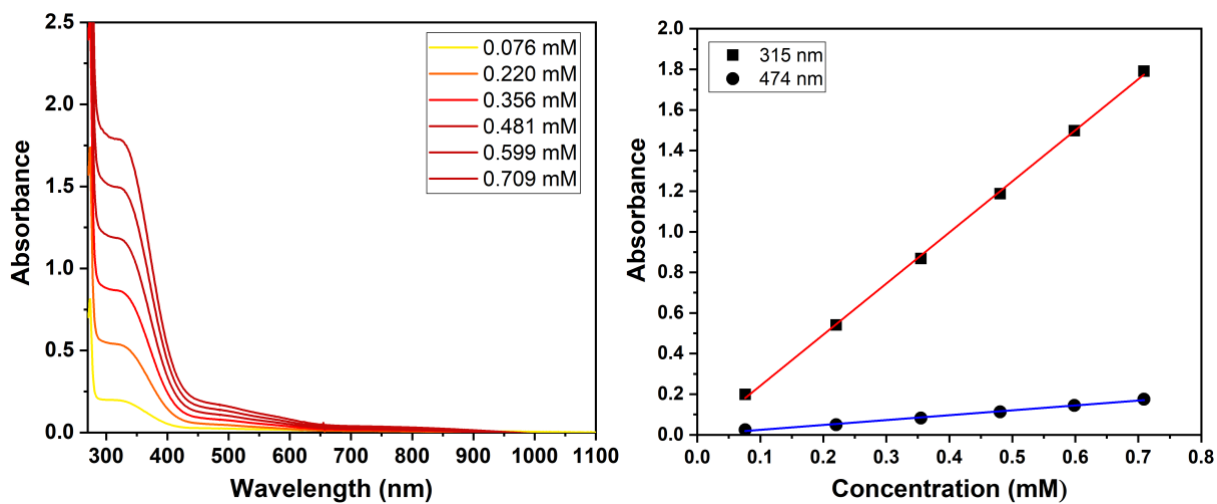


Figure S4: UV-vis spectra of **2** in DCM at various concentration (left) with corresponding Beer's law plot (right).

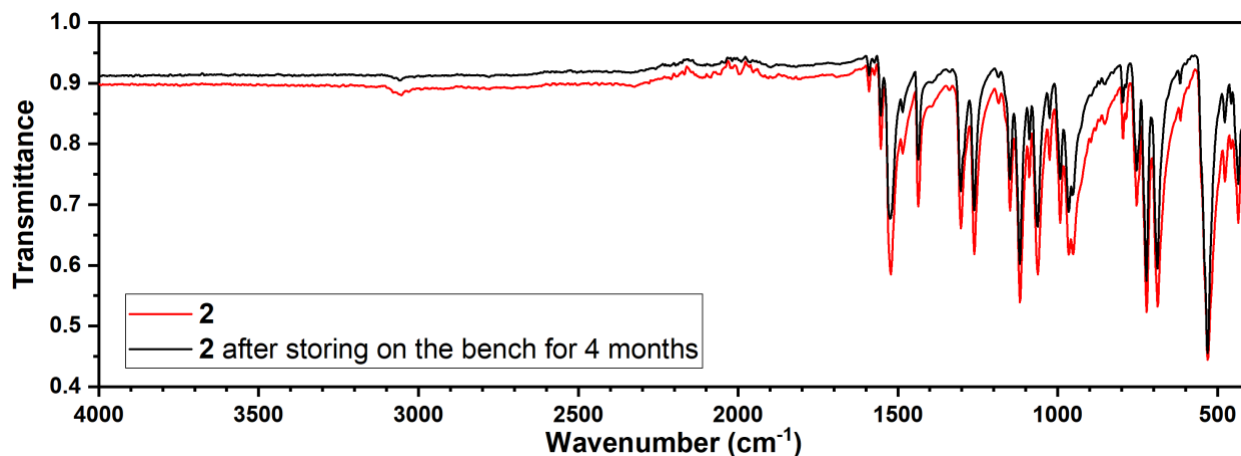


Figure S5: FTIR spectra of crude **2** before and after storing in a scintillation vial on the bench for 4 months at room temperature.

Synthesis and characterization of $[Mn(NO_3)_3(OAsPh_3)_2]$ (**4**)

One-pot synthesis: In 20 mL scintillation vial equipped with a stir bar, $AgNO_3$ (516 mg, 3.04 mmol, 16 eq.) was dissolved in 3 mL MeCN and Me_3SiCl (0.381 mL, 3.04 mmol, 16 eq.) was added dropwise under constant stirring to generate Me_3SiONO_2 *in-situ*. $KMnO_4$ (30.0 mg, 0.190 mmol, 1.0 eq.) and $Mn(OAc)_2$ (131 mg, 0.759 mmol, 4.0 eq.) were stirred in 5 mL MeCN in another 20 mL scintillation vial. The Me_3SiONO_2 solution was filtered (15 mL glass frit with celite) directly into the second mixture to give brown solution **3**; 1 mL of MeCN was used to wash any remaining Me_3SiONO_2 into the reaction flask through the frit. After 15 minutes of stirring, Ph_3AsO (489 mg, 1.52 mmol, 8.0 eq.) was added to the reaction mixture. The reaction mixture turns deep purple brown and was allowed to stir at room temperature for 1.5 hours during which a deep purple precipitate form. The precipitate was filtered out and washed with minimal amount of MeCN and Et_2O then dried under vacuum to obtain **4** as a bright purple solid. The crude product was dissolved in DCM, the saturated solution filtered over a small celite plug, and layered under pentanes at room temperature yielded deep purple crystals of **4** which were washed with pentane and dried under vacuum to yield crystalline **4** (408 mg, 61%).

From 2: In a 20 mL scintillation vial equipped with a stir bar, **2** (100 mg, 0.125 mmol, 1.0 eq.) was dissolved in 4 mL THF to give a yellow brown solution. Ph_3AsO (80.8 mg, 0.251 mmol, 2.0 eq.) was added to the reaction mixture under constant stirring to cause an immediate color change to deep purple along with formation of a purple precipitate. The reaction mixture was left to stir at room temperature for 45 minutes. The reaction mixture was filtered through a fine frit and the solid washed with 2 mL THF then dried under vacuum to isolate **4** as a bright purple solid. The crude product was dissolved in DCM, the saturated solution filtered over a small celite plug, layered under pentane at room temperature to yield deep purple crystals of **4**. The crystals were washed with pentane and dried under vacuum to yield crystalline **4** (65.9 mg, 60%).

ATR-FTIR (cm^{-1}): 3061, 1508, 1471, 1440, 1300, 1271, 1083, 1022, 997, 898, 851, 754, 737, 685, 501, 478, 467, 451.

1H -NMR (CD_3CN): 8.45, 7.30.

Evans' method (dichloromethane- d_2 , 500 MHz, 298 K) $\mu_{eff} = 5.33 \mu_B$.

CHN [Calc. (found)] for $(C_{36}H_{30}MnN_3O_{11}As_2)$: % C 48.83 (48.81), % H 3.42 (3.38), % N 4.75 (4.52).

UV-vis λ_{max} [DCM, (ϵ , $M^{-1}cm^{-1}$)]: 300 (4800), 530 (290).

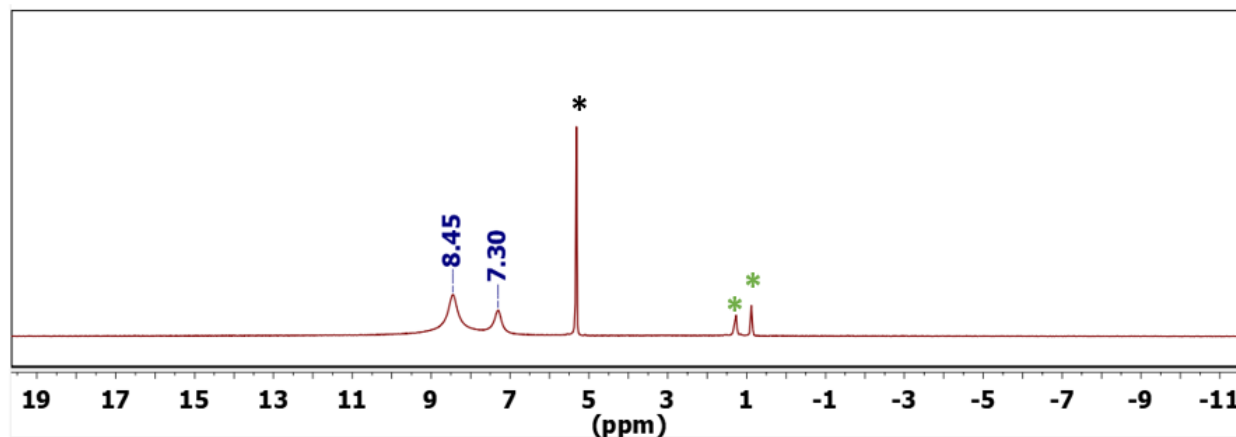


Figure S6: 1H -NMR spectrum of **4** in CD_2Cl_2 (*). * denotes hexanes.

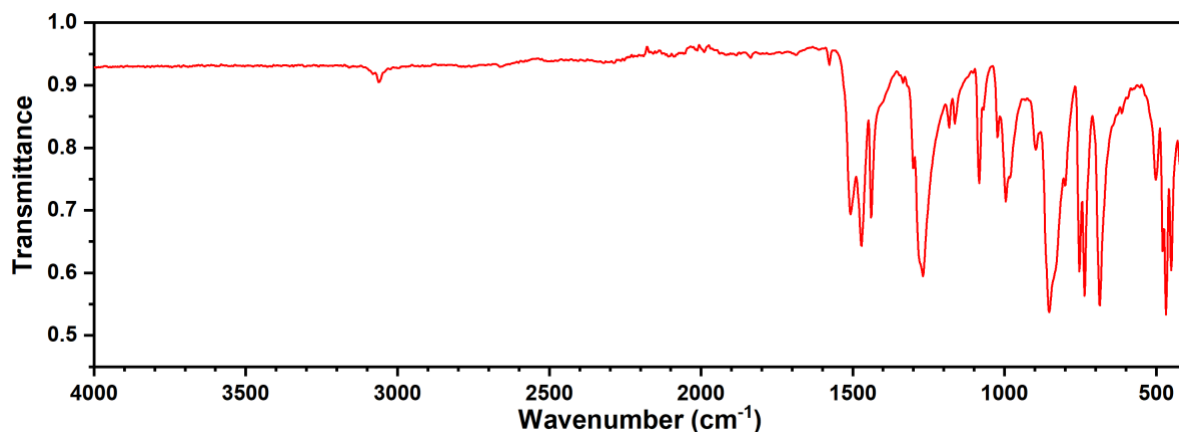


Figure S7: ATR-FTIR spectrum of **4**.

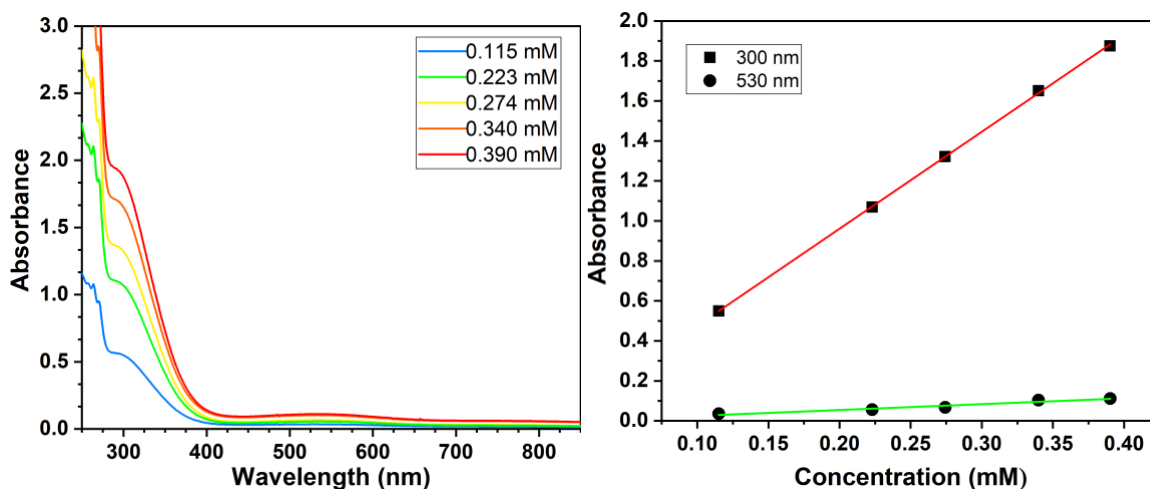


Figure S8: UV-vis spectra of **4** in DCM at various concentration (left) with corresponding Beer's law plot (right).

Synthesis and characterization of $[Mn(NO_3)(MeCN)(Opy)_4][Mn(NO_3)_4]$ (**5**)

One-pot synthesis: In a 20 mL scintillation vial equipped with a stir bar, $AgNO_3$ (258 mg, 1.52 mmol, 16 eq.) was dissolved in 3 mL MeCN and Me_3SiCl (0.191 mL, 1.52 mmol, 16 eq.) was added dropwise under constant stirring to generate Me_3SiONO_2 *in-situ*. $KMnO_4$ (15.0 mg, 0.0949 mmol, 1.0 eq.) and $Mn(OAc)_2$ (65.7 mg, 0.380 mmol, 4.0 eq.) was stirred in 5 mL MeCN in another 20 mL scintillation vial. The Me_3SiONO_2 solution was filtered (15 mL glass frit with celite) directly into the second mixture to give brown solution **3**; 1 mL of MeCN was used to wash any remaining Me_3SiONO_2 into the reaction flask through the frit. After 15 minutes of stirring, Opy (72.2 mg, 0.759 mmol, 8 eq.) was added to the reaction mixture. The reaction mixture turns deep red and was allowed to stir for 1.5 hours. The reaction mixture was filtered, and all volatiles were removed under vacuum to obtain a red residue. The residue was dissolved in minimal amount of MeCN and layered with toluene at room temperature to yield crystals of **5**. The crystals were washed with toluene, pentane, and dried under vacuum to yield crystalline **5** (103 mg, 64%).

From 2: In a 20 mL scintillation vial equipped with a stir bar, **2** (200 mg, 0.251 mmol, 1.0 eq.) was dissolved in 4 mL DCM to give a red brown solution. Opy (47.7 mg, 0.502 mmol, 2.0 eq.) was added to the reaction mixture under constant stirring to cause an immediate color change to deep red along with formation of a brown precipitate. The reaction mixture was left to stir at room temperature overnight. The reaction mixture was filtered through a fine frit and precipitate washed with 2 mL DCM and dried under vacuum to isolate a brown solid. The solid was dissolved in minimal of MeCN and layered with toluene at room temperature overnight to yield crystals of **5**. The crystals were washed with toluene, pentane, and dried under vacuum to yield crystalline **5** (28.4 mg, 67%).

ATR-FTIR (cm^{-1}): 3123, 1452, 1437, 1318, 1289, 1197, 1030, 1019, 863, 826, 816, 772, 739, 669, 595, 536, 451, 435, 423.

1H -NMR (CD_3CN): 2.04, 15.88.

CHN [Calc. (found)] for $(C_{22}H_{23}Mn_2N_{10}O_{19}) \cdot 0.1C_7H_8$: % C 32.05 (32.24), % H 2.82 (2.81), % N 16.47 (16.71).

UV-vis λ_{max} [MeCN, nm (ϵ , $M^{-1}cm^{-1}$)]: 275 (29000), 375 (4600), 500 (540).

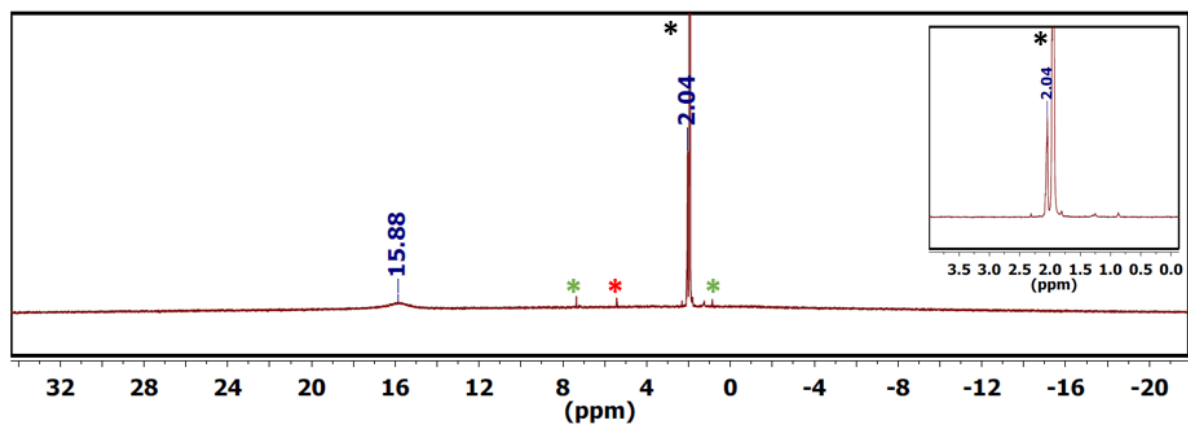


Figure S9: $^1\text{H-NMR}$ spectrum of **5** in CD_3CN (*). * and * denotes toluene and DCM respectively. Insert: magnification of spectrum at 0.0-4.0 ppm.

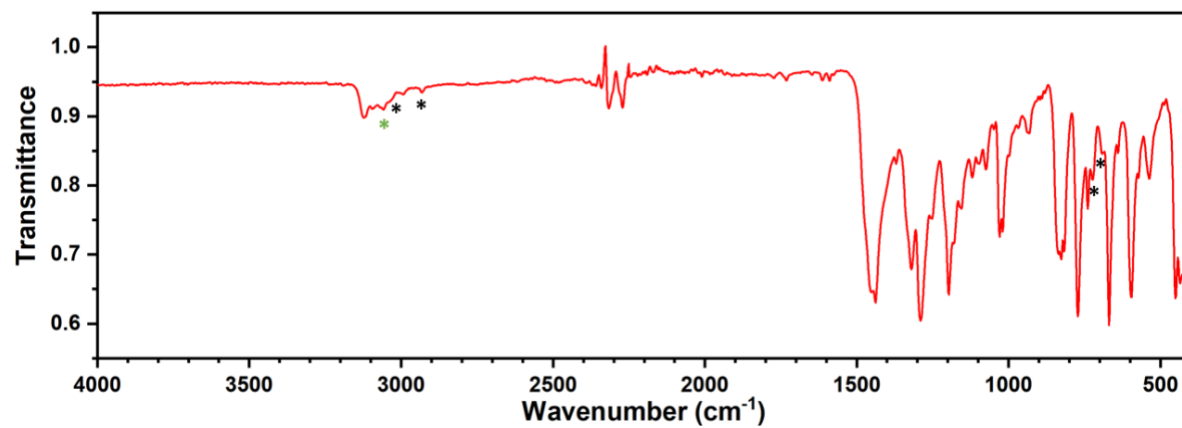


Figure S10: ATR-FTIR spectrum of **5**. * and * denotes toluene and DCM respectively.

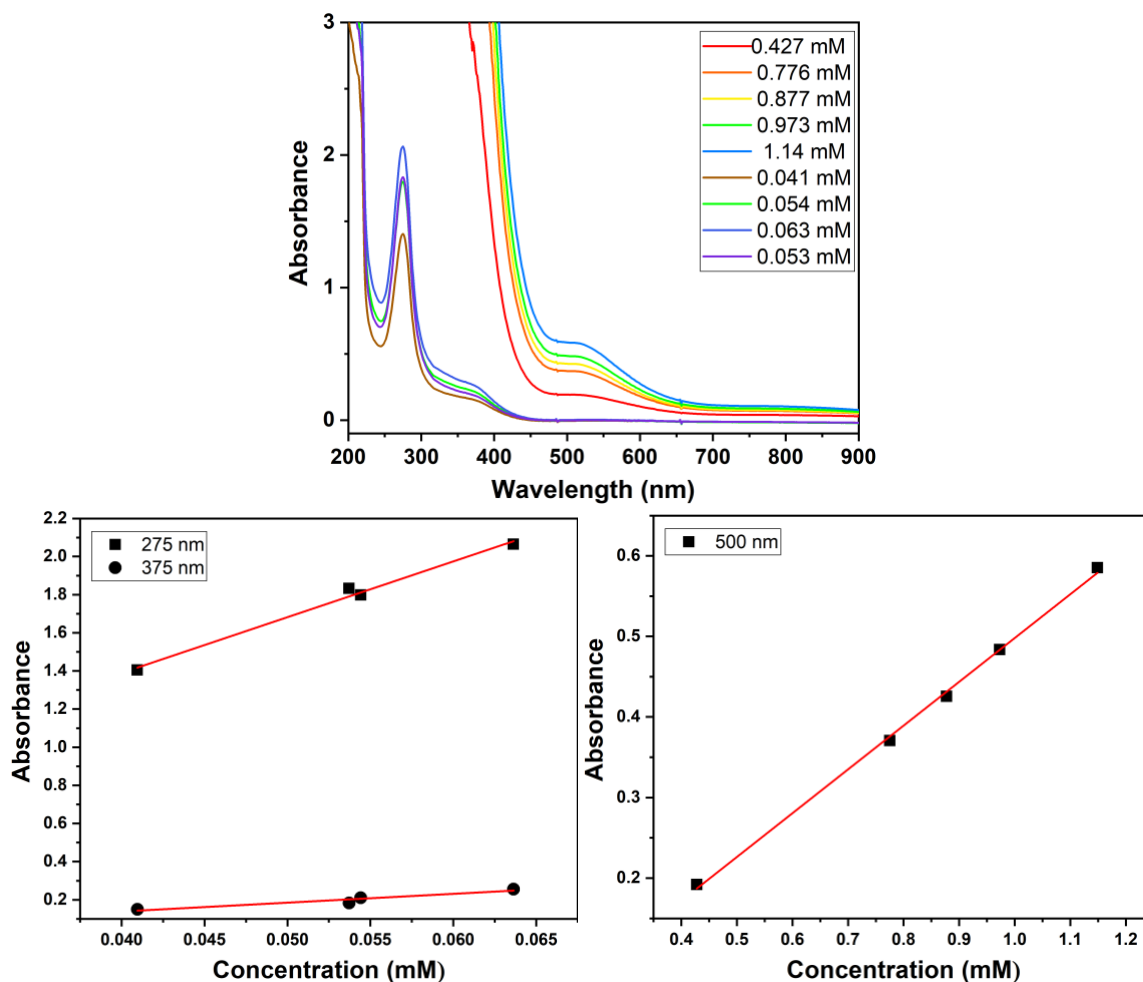


Figure S11: UV-vis spectra of **5** in MeCN at various concentration (top) with corresponding Beer's law plot (bottom).

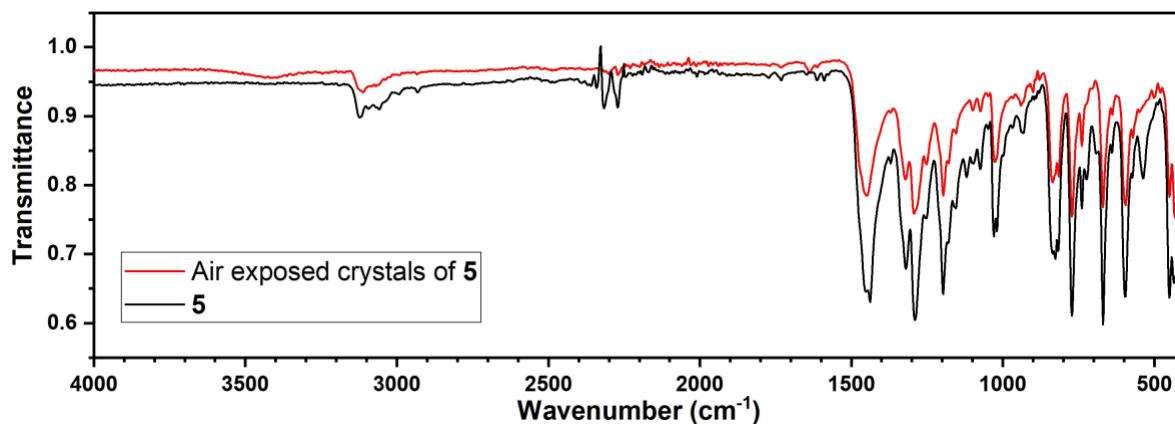


Figure S12: ATR-FTIR spectrum of **5** after exposure to air for 16 h. A new peak at 4310 cm^{-1} appears upon exposure of crystals of **5** to air.

Synthesis and characterization of $[\text{MnCl}_2(\text{NO}_3)(\text{OPPh}_3)_2]$ (**6**)

From **2** and **1**: In a 20 mL scintillation vial equipped with a stir bar, **1** (100 mg, 0.139 mmol, 2.0 eq.) was dissolved in 4 mL DCM to give a deep blue solution. **2** (55.5 mg, 0.0696 mmol, 1.0 eq.) was added to the reaction mixture under constant stirring to cause an immediate color change to deep purple. The reaction mixture was left to stir at room temperature for 1 hour. The reaction mixture was then filtered through a fine frit and the filtrate layered under pentane at room temperature to yield purple crystals of **6**. The crystals were washed with pentane and dried under vacuum to yield crystalline **6** (122 mg, 79%). This material was used for all characterization except X-ray diffraction.

From 1: In a 20 mL scintillation vial equipped with a stir bar, AgNO_3 (106 mg, 0.627 mmol, 1.5 eq.) was dissolved in 2 mL MeCN and Me_3SiCl (0.0787 mL, 0.627 mmol, 1.5 eq.) was added dropwise under constant stirring to generate $\text{Me}_3\text{SiONO}_2$ *in-situ*. In another 20 mL scintillation vial equipped with a stir bar, **1** (300 mg, 0.418 mmol, 1.0 eq.) was dissolved in 2 mL MeCN to give a deep blue solution. The $\text{Me}_3\text{SiONO}_2$ solution was filtered through celite and added to reaction mixture under constant stirring (1 mL of MeCN was used to wash any remaining $\text{Me}_3\text{SiONO}_2$ into the reaction flask) causing an immediate color change to purple along with precipitation of a purple solid. The reaction mixture was left to stir for 30 minutes at room temperature. The reaction mixture was filtered through a fine frit, the precipitate washed with 2 mL MeCN, and dried under vacuum to isolate **6** as a purple solid (204 mg, 63%). The product was dissolved in DCM, the saturated solution filtered over a small celite plug, layered under pentane at room temperature to yield purple crystals. Single crystals for X-ray analysis were grown for **6** prepared this way and showed that another species, consistent with 10% **9**, co-crystallized with the product. This impurity was not present in batches of **6** prepared from **2** and **1** as evident from analytical purity and spectroscopic analysis.

ATR-FTIR (cm^{-1}): 3058, 1590, 1518, 1485, 1436, 1269, 1174, 1147, 1118, 1092, 992, 795, 748, 721, 688, 533, 445, 430.

$^1\text{H-NMR}$ (CD_2Cl_2): 8.78, 7.19.

Evans' method (dichloromethane $-d_2$, 500 MHz, 298 K) $\mu_{\text{eff}} = 5.10 \mu\text{B}$.

CHN [Calc. (found)] for $(\text{C}_{36}\text{H}_{30}\text{Cl}_2\text{MnNO}_5\text{P}_2) \cdot 0.3\text{CH}_2\text{Cl}_2$: % C 56.63 (56.43), % H 4.01 (3.76), % N 1.82 (2.13).

UV-vis λ_{max} [DCM, nm (ϵ , $\text{M}^{-1}\text{cm}^{-1}$): 310 (2400), 350 (2000), 560 (320).

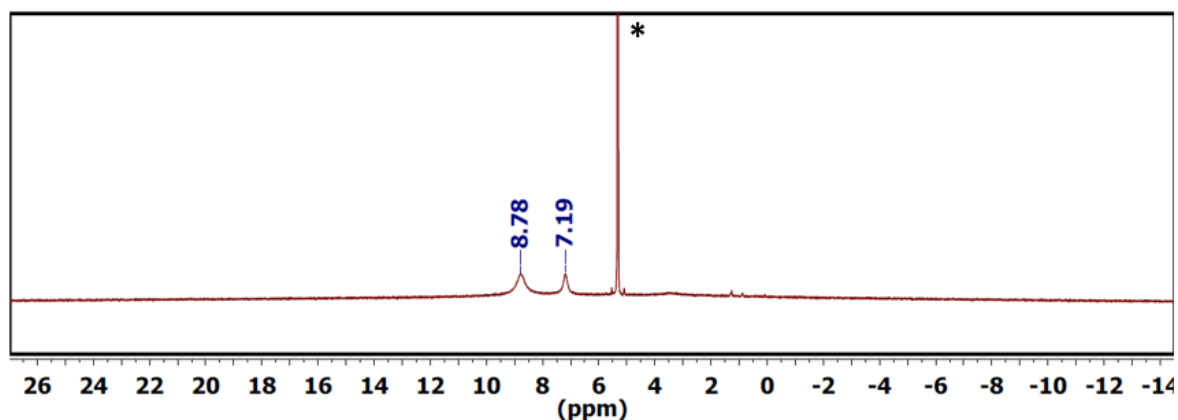


Figure S13: $^1\text{H-NMR}$ spectrum of **6** in CD_2Cl_2 (*).

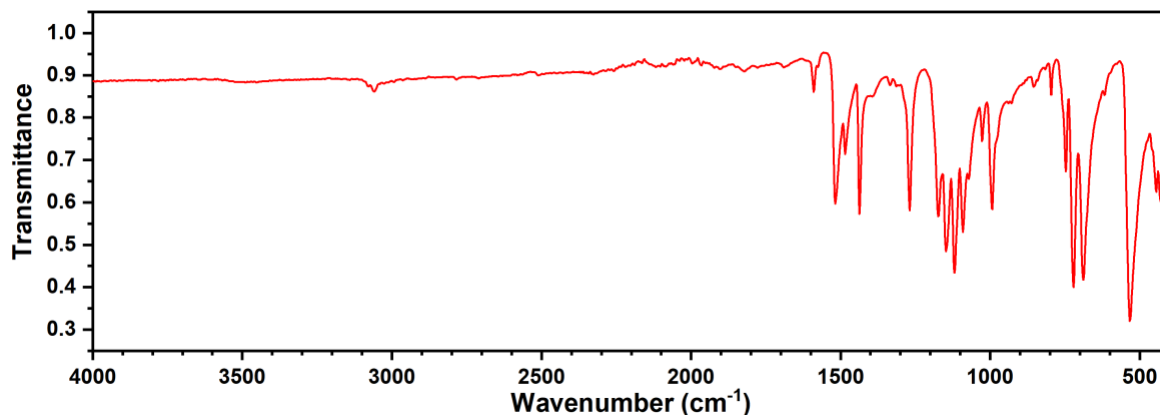


Figure S14: ATR-FTIR spectrum of **6**.

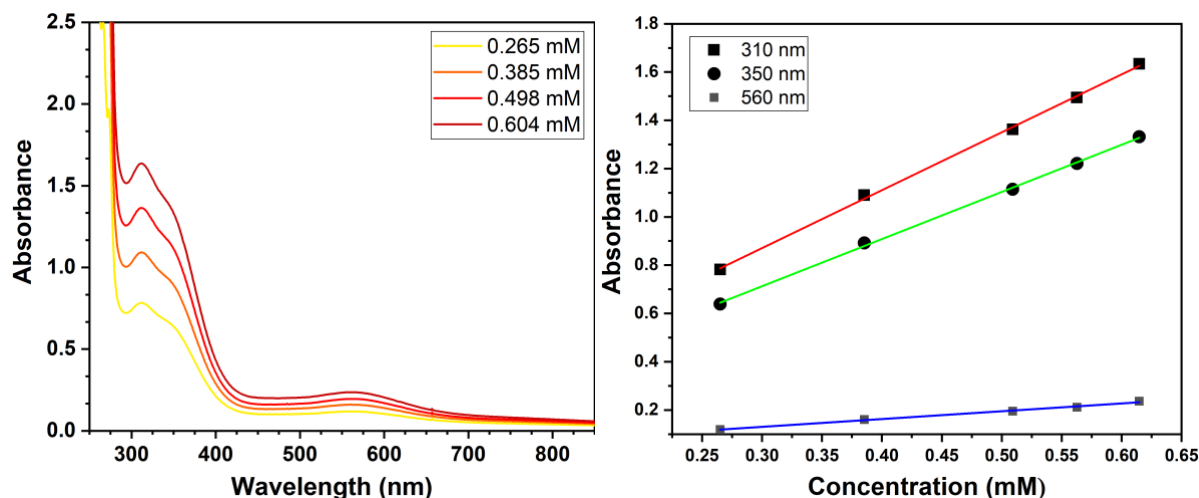


Figure S15: UV-vis spectra of **6** in DCM at various concentration (left) with corresponding Beer's law plot (right).

Synthesis and characterization of $[MnCl_3(OAsPh_3)_2]$ (**7**)

From 1: This reaction may be performed open to air. In a 20 mL scintillation vial equipped with a stir bar, **1** (300 mg, 0.418 mmol, 1.0 eq.) was dissolved in 15 mL THF to give a purple blue solution. Ph_3AsO (269 mg, 0.836 mmol, 2.0 eq.) was added to the reaction mixture under constant stirring to cause an immediate color change to deep blue along with precipitation of a bright blue solid. The reaction mixture was left to stir at room temperature for 15 minutes. The reaction mixture was filtered through a fine frit, and precipitate washed with 2 mL THF, and dried under vacuum to isolate **7** as a bright blue solid (304 mg, 90%).

From Mn_{12} : Mn_{12} (40.0 mg, 0.0194 mmol, 1.0 eq.) was stirred in 3 mL MeCN in a 20 mL scintillation vial to give an intense coffee brown solution. Me_3SiCl (0.0878 mL, 0.699 mmol, 36 eq.) was added dropwise via syringe with vigorous stirring to give a deep purple solution. Ph_3AsO (150 mg, 0.466 mmol, 24 eq.) was added to the reaction mixture, which immediately turns deep blue and forms of a bright blue precipitate. After 30 minutes of stirring at room temperature, the reaction mixture was filtered through a fine frit to isolate **7** as a bright blue solid. The solid was washed with minimal amount of MeCN, Et_2O , and dried under vacuum. The crude product was dissolved in DCM, the saturated solution filtered over a small celite plug, layered under pentane at room temperature to yield deep blue crystals of **7**. The crystals were washed with pentane and dried under vacuum to yield crystalline **7** (138 mg, 74%).

ATR-FTIR (cm^{-1}): 3054, 1577, 1480, 1442, 1332, 1310, 1182, 1161, 1083, 1023, 995, 830, 752, 739, 686, 503, 478, 463, 453.

1H -NMR ($CDCl_3$): 8.29, 7.63.

Evans' method (dichloromethane- d_2 , 500 MHz, 298 K) $\mu_{eff} = 5.24 \mu_B$.

CHN [Calc. (found)] for $(C_{36}H_{30}Cl_3Mn_2As_2O_2) \cdot 0.5CH_2Cl_2$: % C 51.68 (51.38), % H 3.68 (3.70).

UV-vis λ_{max} [DCM, nm (ϵ , $M^{-1}cm^{-1}$): 345 (2200), 690 (770).

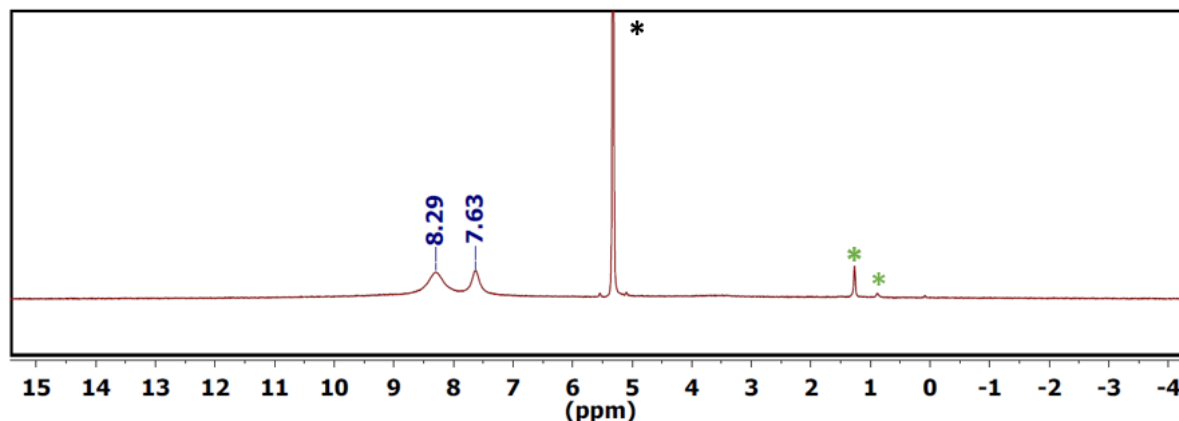


Figure S16: 1H -NMR spectrum of **7** in CD_2Cl_2 (*). * denotes hexanes.

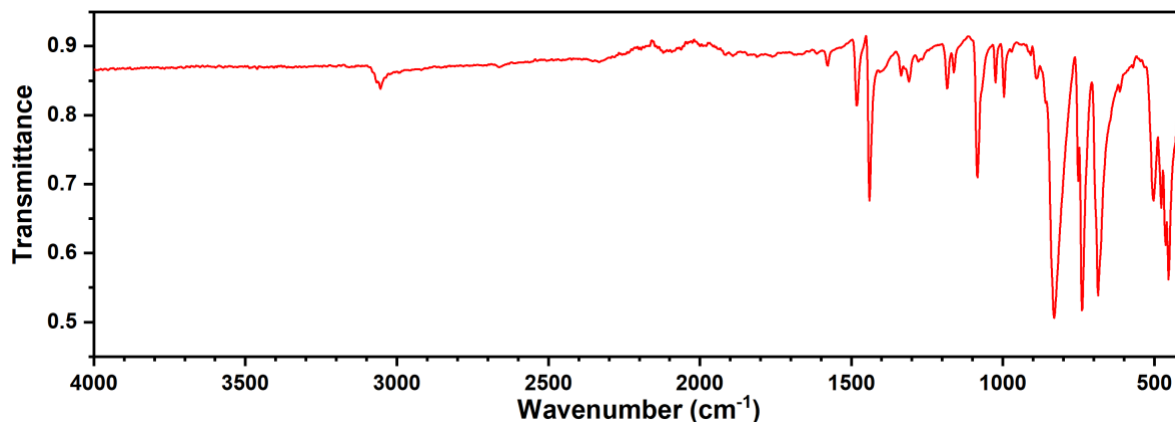


Figure S17: ATR-FTIR spectrum of **7**.

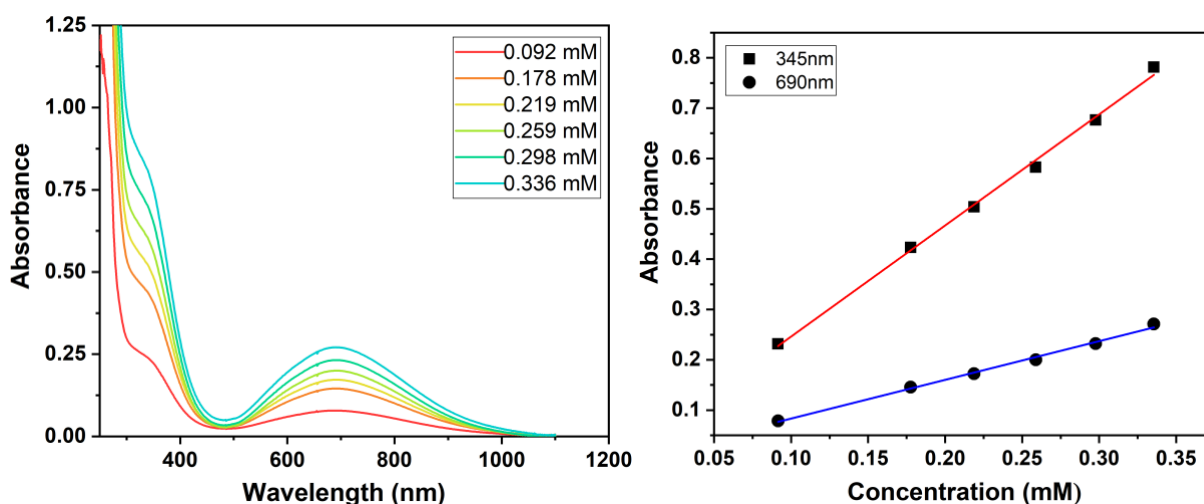


Figure S18: UV-vis spectra of **7** in DCM at various concentration (left) with corresponding Beer's law plot (right).

Synthesis and characterization of $[MnCl_2(NO_3)(OAsPh_3)_2]$ (**8**)

From 4 and 7: In a 20 mL scintillation vial equipped with a stir bar, **7** (70 mg, 0.0869 mmol, 2.0 eq.) was dissolved in 3 mL DCM to give a bright blue solution. **4** (38.5 mg, 0.0434 mmol, 1.0 eq.) was added to the reaction mixture under constant stirring to cause an immediate color change to deep purple. The reaction mixture was left to stir at room temperature for 1 hour. The reaction mixture was then filtered through a fine frit and layered under pentane at room temperature to yield deep blue-purple crystals of **8**. The crystals were washed with pentane and dried under vacuum to yield crystalline **8** (99.2 mg, 92%). This material was used for all characterization except X-ray diffraction.

From 7: In a 20 mL scintillation vial equipped with a stir bar, $AgNO_3$ (14.8 mg, 0.0869 mmol, 1 eq.) was dissolved in 2 mL MeCN and Me_3SiCl (0.0109 mL, 0.0869 mmol, 1.0 eq.) was added dropwise under constant stirring to generate Me_3SiONO_2 *in-situ*. In another 20 mL scintillation vial equipped with a stir bar, **7** (70.0 mg, 0.0869 mmol, 1.0 eq.) was stirred in 2 mL MeCN to give a deep blue turbid mixture. The Me_3SiONO_2 solution was filtered through celite and added to reaction mixture under constant stirring and caused an immediate color change to deep purple. The reaction mixture was left to stir for 30 minutes. The solvent from reaction mixture was removed under vacuum to obtain a deep purple oil. The oil was dissolved in 1 mL DCM and layered under pentanes to give **8** as purple crystals which were washed with pentanes and dried under vacuum (30.1 mg, 43%). The product was dissolved in DCM, the saturated solution filtered over a small celite plug, layered under pentane at room temperature to yield deep blue-purple crystals. Single crystals for X-ray analysis were grown for **8** prepared this way and showed that some **7** co-crystallized with the product. **7** was not present in batches of **8** prepared from **4** and **7** as evident from analytical purity and spectroscopic analysis.

ATR-FTIR (cm^{-1}): 3054, 1578, 1475, 1438, 1334, 1308, 1283, 1184, 1159, 1085, 1015, 997, 830, 748, 737, 686, 505, 472, 463, 447, 426.

1H -NMR (CD_2Cl_2): 8.48, 7.30.

Evans' method (dichloromethane- d_2 , 400 MHz, 298 K) $\mu_{eff} = 4.84 \mu_B$.

CHN [Calc. (found)] for (C₃₆H₃₀Cl₂MnNO₅As₂): % C 51.95 (51.99), % H 3.63 (3.67), % N 1.68 (1.67).
UV-vis λ_{max} [DCM, nm (ϵ , M⁻¹cm⁻¹): 255 (13000), 310 (3400), 590 (370).

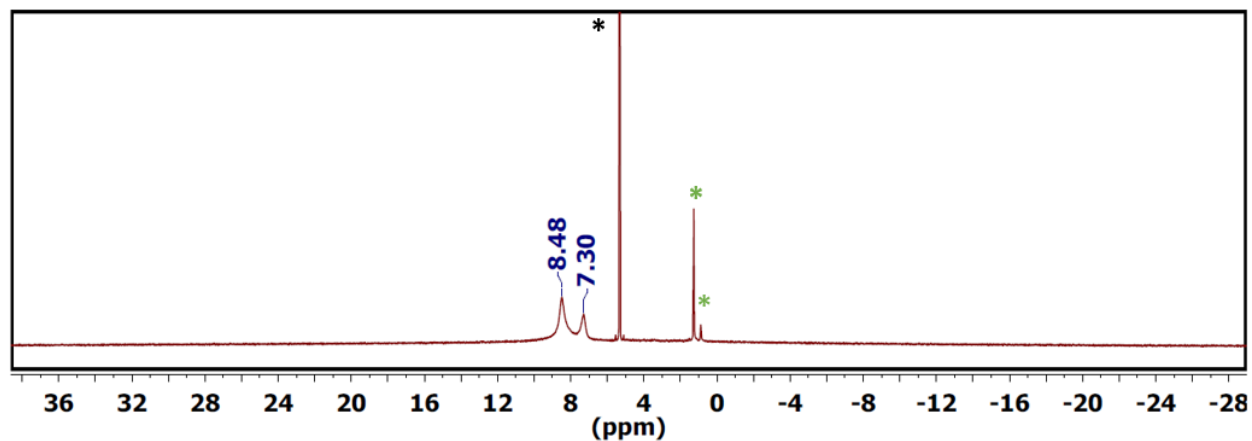


Figure S19: ¹H-NMR spectrum of **8** in CD₂Cl₂ (*). * denotes pentanes.

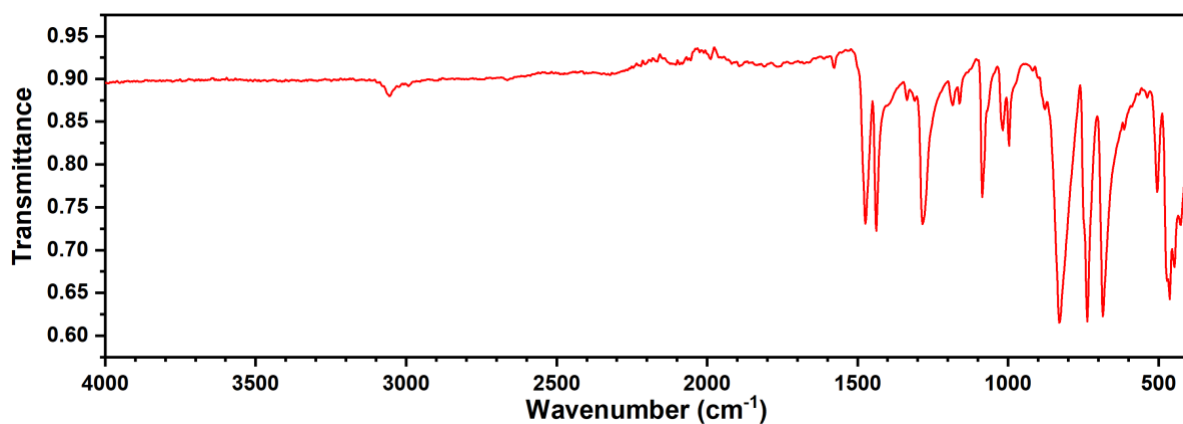


Figure S20: ATR-FTIR spectrum of **8**.

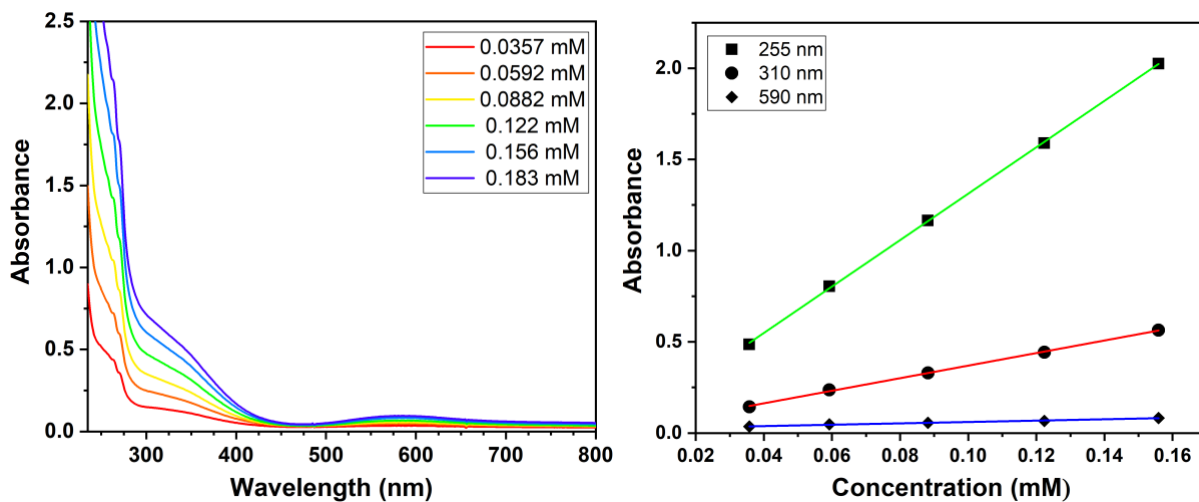


Figure S21: UV-vis spectra of **8** in DCM at various concentration (left) with corresponding Beer's law plot (right).

Characterization of $[Mn(NO_3)_2(OPPh_3)_2]$ (**9**)

CHN [Calc. (found)] for $(C_{36}H_{30}MnN_2O_8P_2)$: % C 58.79 (58.34), % H 4.11 (4.11), % N 3.81 (3.71).

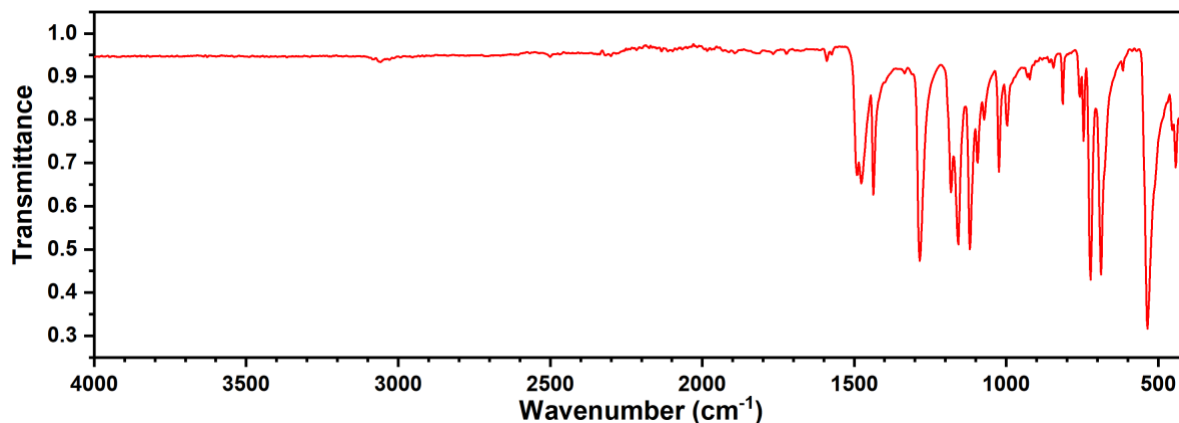


Figure S22: ATR-FTIR spectrum of **9**.

EPR spectra of selected complexes

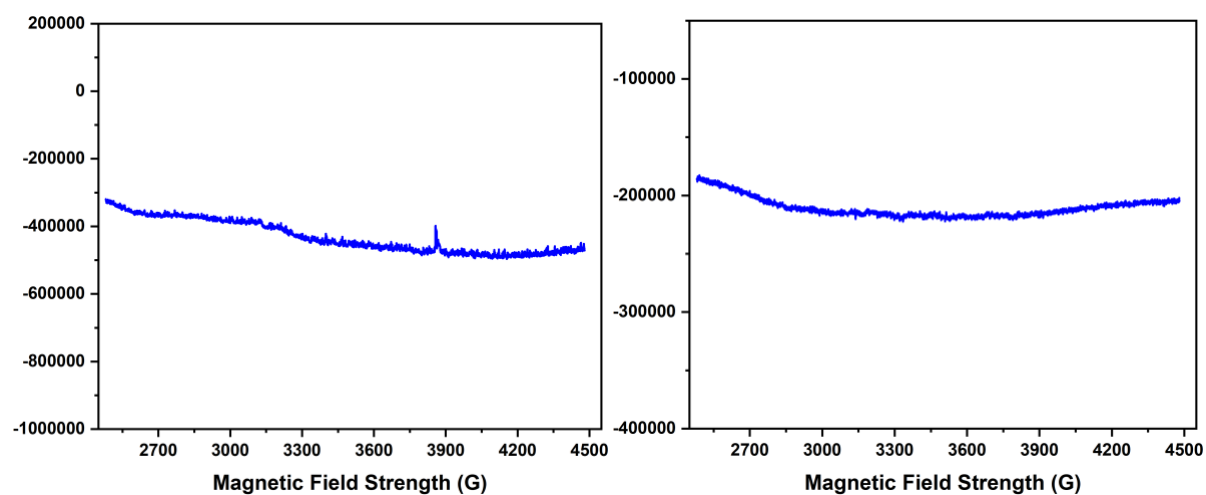


Figure S23: Perpendicular mode X-Band EPR spectra of 2.5 mM **2** (left) and **4** (right) in 9:1 DCM:toluene at 77 K.

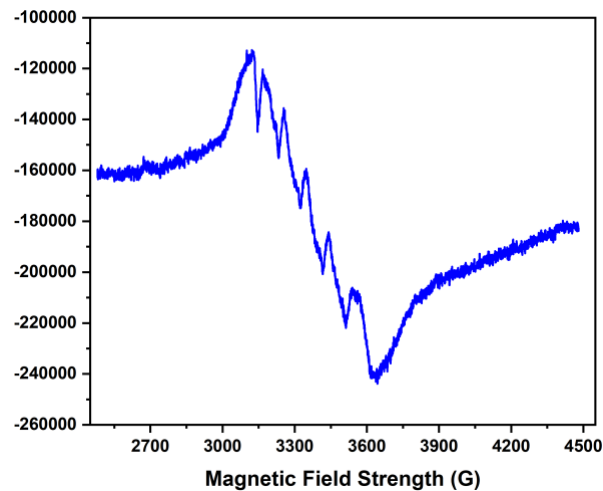


Figure S24: Perpendicular mode X-Band EPR spectrum of 2.5 mM **9** in 9:1 DCM:toluene at 77 K.

Determining solubility of **2** in fluorobenzene

Molar absorption coefficient of **2** in fluorobenzene was determined by constructing a Beer's law plot using a dilute stock solution (0.9 mM).

UV-vis λ_{\max} [fluorobenzene, nm (ϵ , $M^{-1}cm^{-1}$): 320 (3200), 480 (370).

A saturated solution of **2** in fluorobenzene was prepared and absorbance of a diluted aliquot was collected to determine the solubility. Average solubility from two trials : 8.32 mg/mL

Note: ACS Grade fluorobenzene was degassed by 4 freeze-pump-thaw cycles, stored under 3 Å molecular sieves for 24h in an inert atmosphere, and further dried by passing through a plug of dried basic alumina before use.

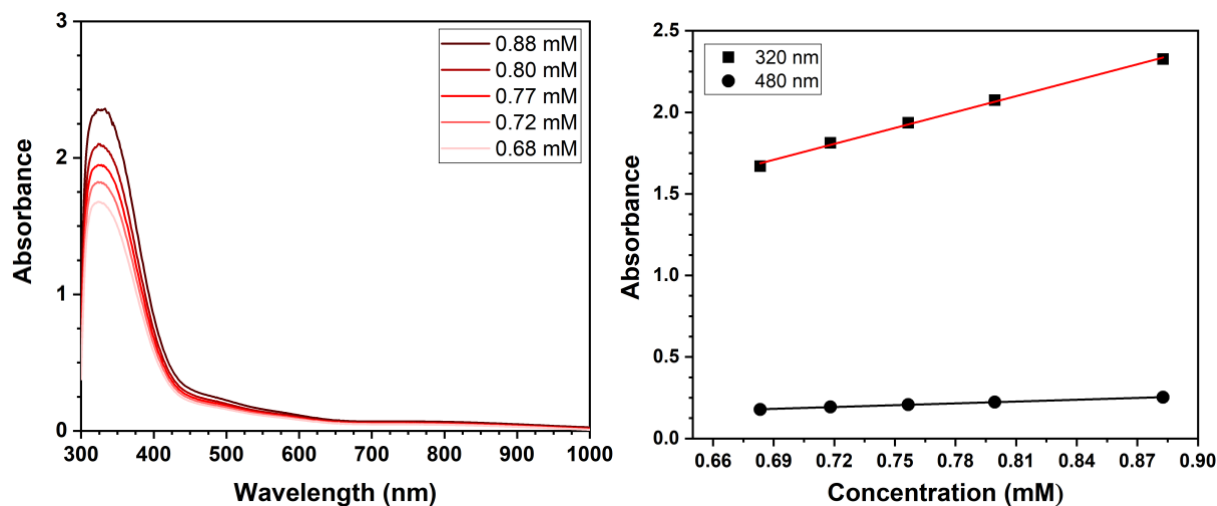


Figure S25: UV-vis spectra of **2** in fluorobenzene at various concentration (left) with corresponding Beer's law plot (right).

Electrochemistry Experiments

The Mn^{III}/Mn^{II} reduction potentials of Mn(III) complexes were determined using cyclic voltammetry and differential pulse voltammetry experiments. The electrochemical cell was equipped with a glassy carbon working electrode, Ag/Ag^+ (4-8 mM $AgBF_4$ in DCM or 4-8 mM $AgNO_3$ in MeCN, 0.5 M $[nBu_4N][PF_6]$) reference electrode with a CoralPor™ separator, and a platinum auxiliary electrode. 0.5 M solution of $[nBu_4N][PF_6]$ was used as the supporting electrolyte; scans were performed with internal resistance compensation (85%). The analyte concentration was 6 mM. Scan direction was cathodic (scan rate: 200 mV/s). The reference electrode was externally referenced to ferrocene at the beginning and end of the experiment. For differential pulse voltammetry, the step height was set to 10 mV, the pulse height was 100 mV, the pulse width was 25 ms, and the step width was 100 ms. Scan direction was cathodic.

Table S1: Electrochemical data for Mn^{III}/Mn^{II} reduction potentials in MeCN

Complex	Potential (V) vs. $FeCp_2$ in MeCN	
	From CV	From DPV
$[Mn(NO_3)_3(OPPh_3)_2]$ (2)	1.020 ± 0.001^a	1.020 ± 0.002^a
$[Mn(NO_3)_3(OAsPh_3)_2]$ (4)	0.950	1.00
$[Mn(OPy)_4(MeCN)(NO_3)][Mn(NO_3)_4]$ (5)	1.02, 0.560	1.02, 0.550
$[MnCl_2(NO_3)(OPPh_3)_2]$ (6)	0.721	0.710
$[MnCl_3(OAsPh_3)_2]$ (7)	0.715	0.756
$[MnCl_2(NO_3)(OAsPh_3)_2]$ (8)	0.678	0.696

(a) From triplicate runs

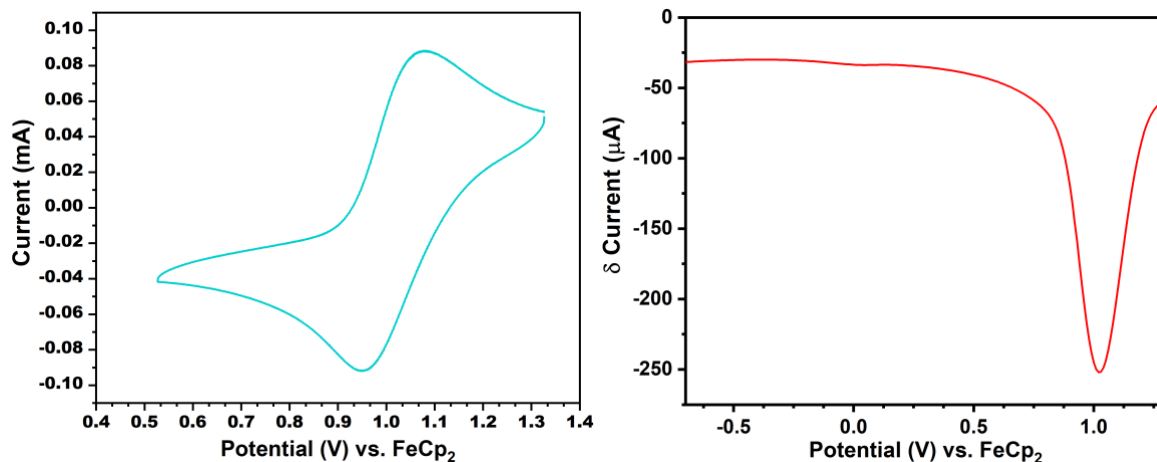


Figure S26: (Left) The cyclic voltammogram (200 mV/s, $i_{pc}/i_{pa} = 0.82$) and (right) differential pulse voltammogram of **2** in 0.5 M $[nBu_4N][PF_6]$ in MeCN.

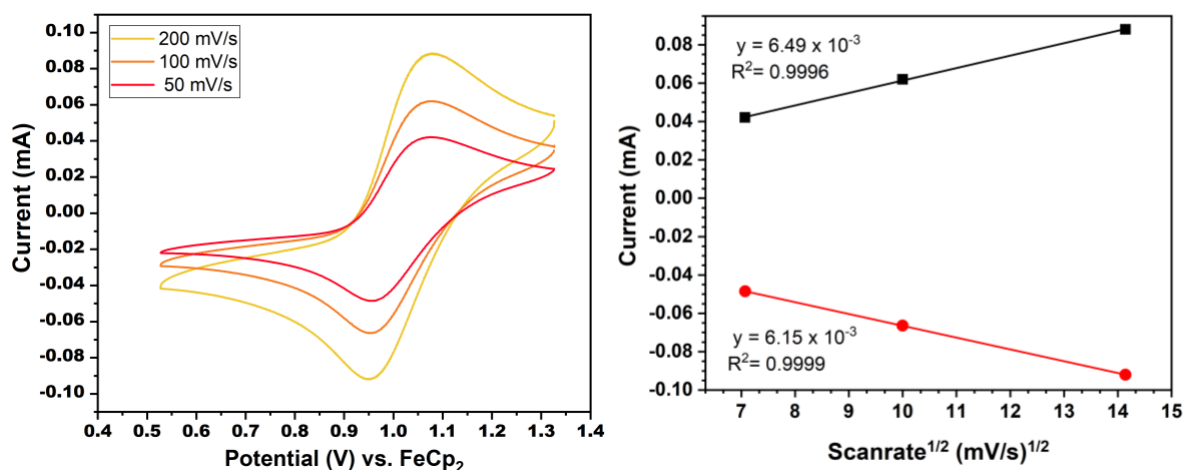


Figure S27: (Left) Cyclic voltammograms of **2** in 0.5 M $[nBu_4N][PF_6]$ in MeCN at varying scan rates. (Right) Peak current vs. $(\text{scan rate})^{1/2}$ with linear fit.

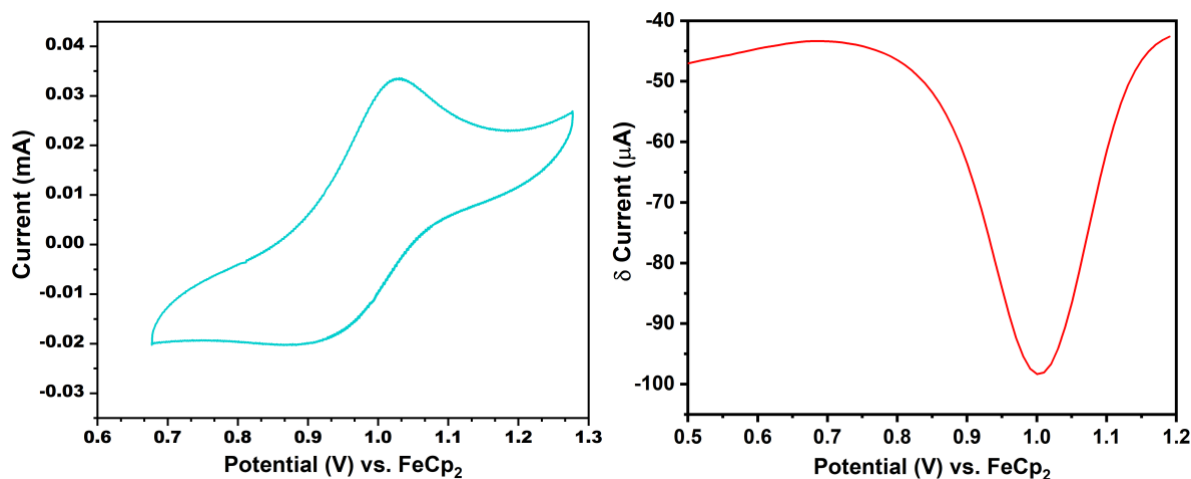


Figure S28: (Left) The cyclic voltammogram (200 mV/s, $i_{pc}/i_{pa} = 0.62$) and (right) differential pulse voltammogram of **4** in 0.5 M $[nBu_4N][PF_6]$ in MeCN.

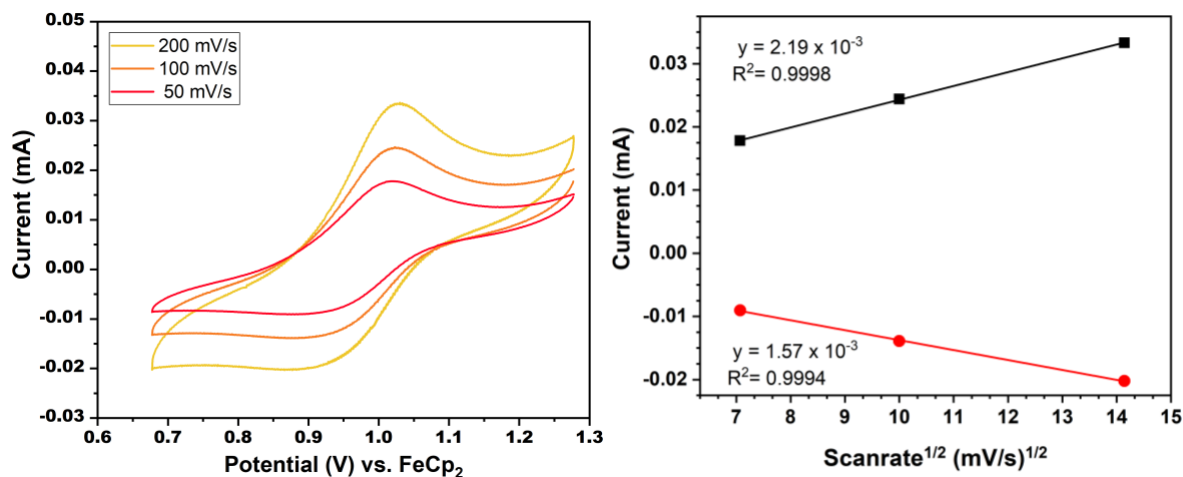


Figure S29: (Left) Cyclic voltammograms of **4** in 0.5 M $[n\text{Bu}_4\text{N}][\text{PF}_6]$ in MeCN at varying scan rates. (Right) Peak current vs. $(\text{scan rate})^{1/2}$ with linear fit.

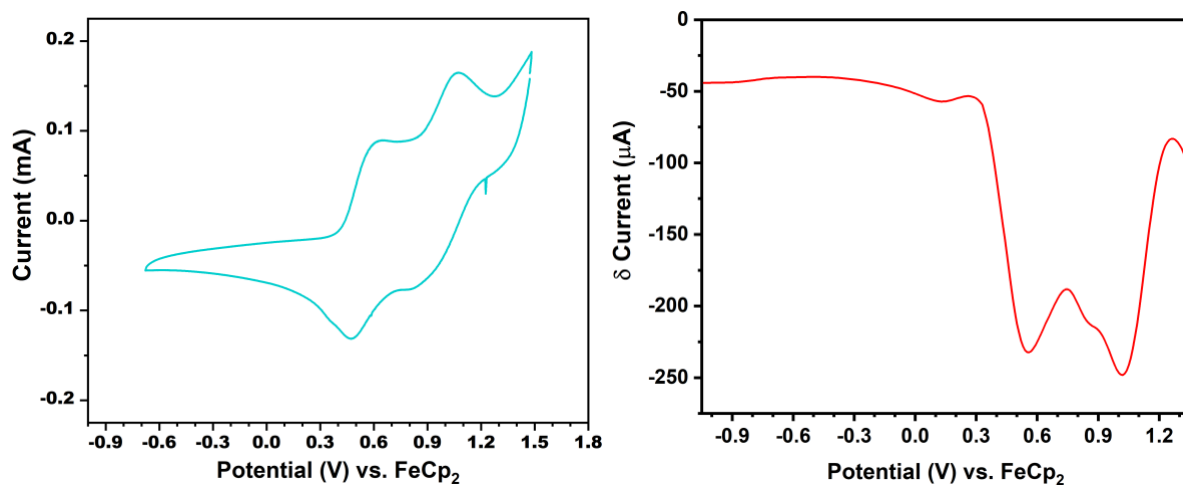


Figure S30: (Left) The cyclic voltammogram (200 mV/s, $i_{\text{pc}}/i_{\text{pa}} = 1.0$ for potential at 1.02 V and $i_{\text{pc}}/i_{\text{pa}} = 0.57$ for potential at 0.560 V) and (right) differential pulse voltammogram of **5** in 0.5 M $[n\text{Bu}_4\text{N}][\text{PF}_6]$ in MeCN. The most positive feature is reported in the manuscript. The solution state speciation was not interrogated further.

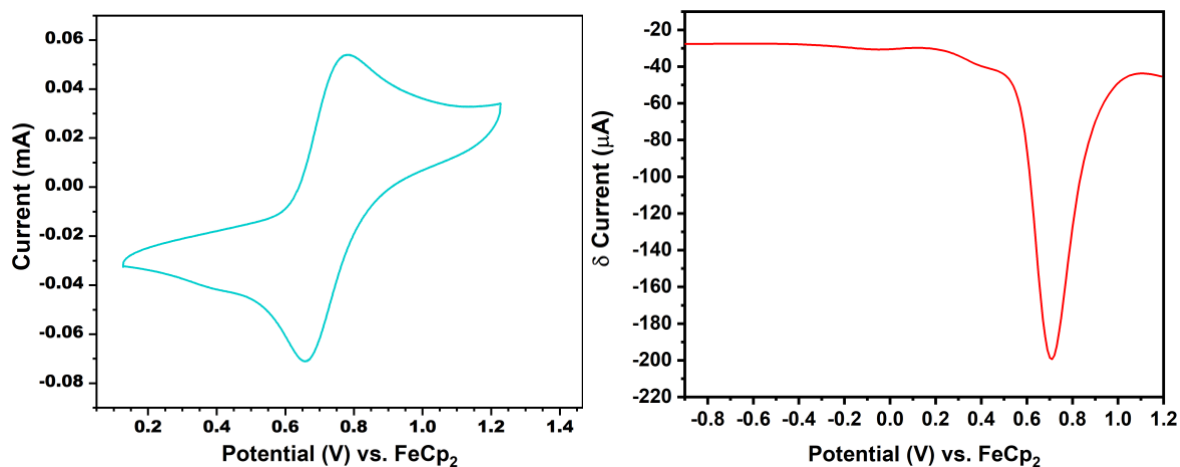


Figure S31: (Left) The cyclic voltammogram (200 mV/s, $i_{\text{pc}}/i_{\text{pa}} = 0.97$) and (right) differential pulse voltammogram of **6** in 0.5 M $[n\text{Bu}_4\text{N}][\text{PF}_6]$ in MeCN.

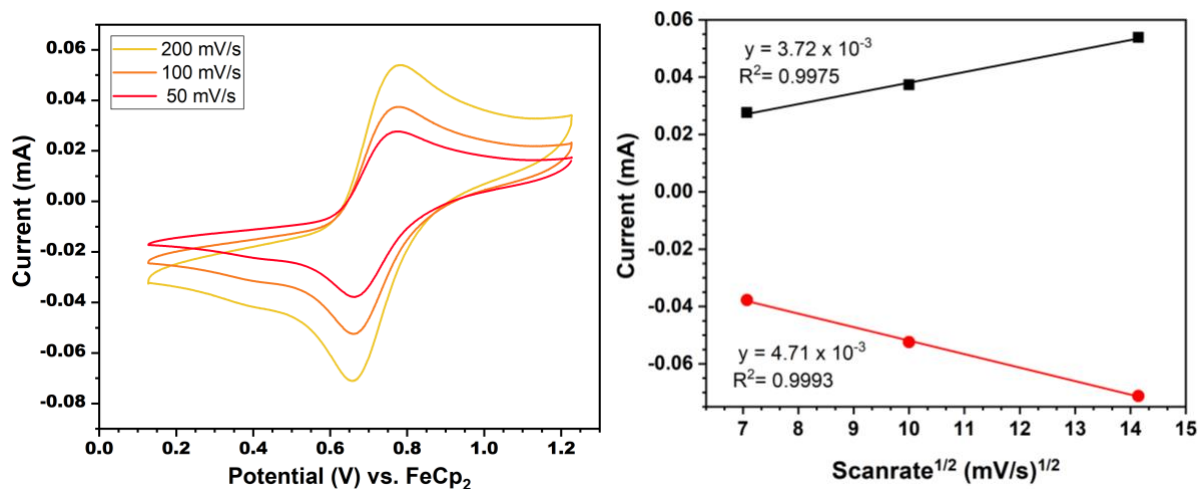


Figure S32: (Left) Cyclic voltammograms of **6** in 0.5 M [nBu₄N][PF₆] in MeCN at varying scan rates. (Right) Peak current vs. (scan rate)^{1/2} with linear fit.

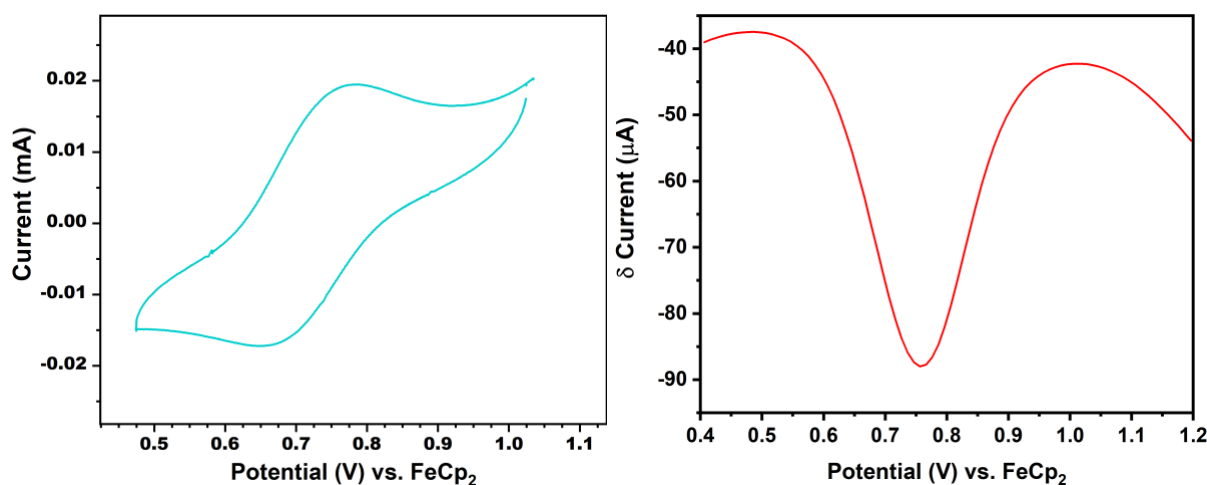


Figure S33: (Left) The cyclic voltammogram (200 mV/s, $i_{pc}/i_{pa} = 0.81$) and (right) differential pulse voltammogram of **7** in 0.5 M [nBu₄N][PF₆] in MeCN.

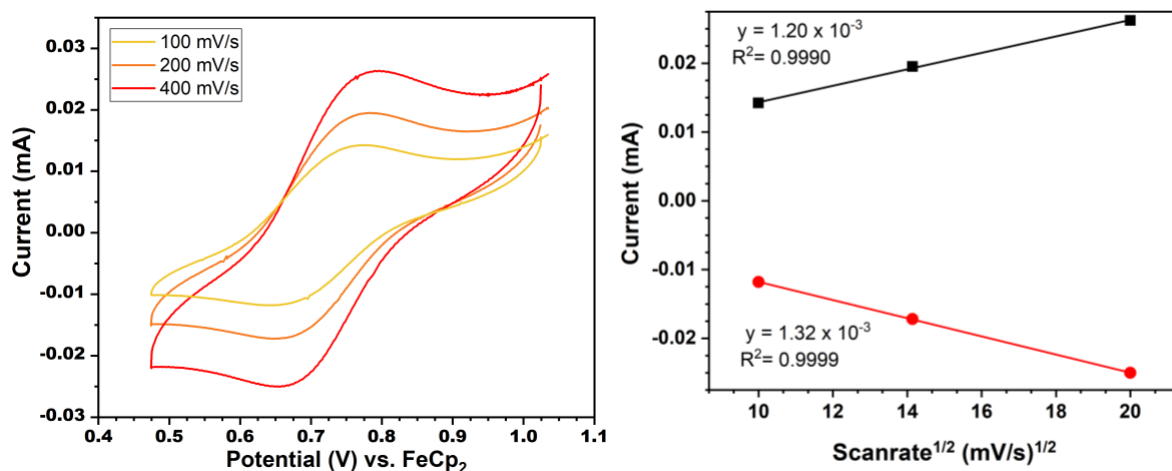


Figure S34: (Left) Cyclic voltammograms of **7** in 0.5 M [nBu₄N][PF₆] in MeCN at varying scan rates. (Right) Peak current vs. (scan rate)^{1/2} with linear fit.

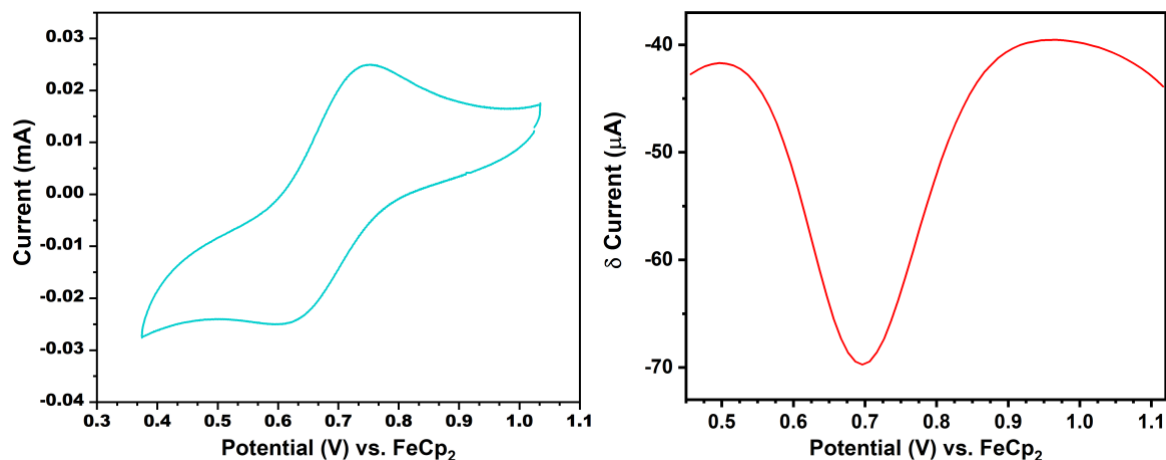


Figure S35: (Left) The cyclic voltammogram (200 mV/s, $i_{pc}/i_{pa} = 0.91$) and (right) differential pulse voltammogram of **8** in 0.5 M $[nBu_4N][PF_6]$ in MeCN.

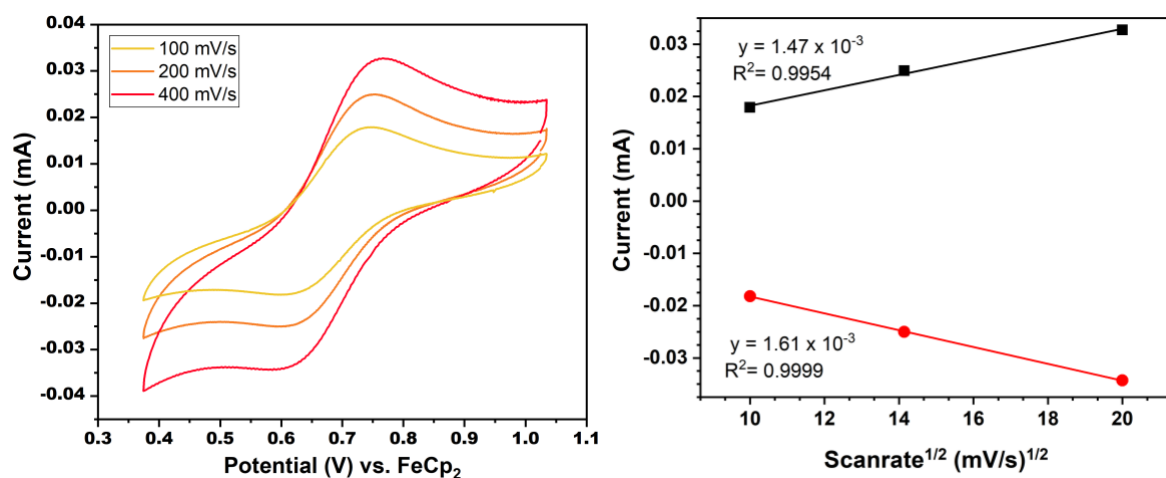


Figure S36: (Left) Cyclic voltammograms of **8** in 0.5 M $[nBu_4N][PF_6]$ in MeCN at varying scan rates. (Right) Peak current vs. $(\text{scan rate})^{1/2}$ with linear fit.

Table S2: Electrochemical data for Mn^{III}/Mn^{II} reduction potentials in DCM

Complex	Potential (V) vs. FeCp ₂ in DCM							
	From CV				From DPV			
	Run 1	Run 2	Run 3	Average	Run 1	Run 2	Run 3	Average
$[Mn(NO_3)_3(OPPh_3)_2]$ (2)	0.963	0.953	0.976	0.964±0.007	0.950	0.955	0.980	0.962±0.009
$[Mn(NO_3)_3(OAsPh_3)_2]$ (4)	0.898	0.914	0.921	0.911±0.007	0.910	0.945	0.955	0.937±0.014
$[MnCl_2(NO_3)(OPPh_3)_2]$ (6)	0.679	0.672	0.677	0.676±0.002	0.690	0.660	0.713	0.688±0.015
$[MnCl_3(OAsPh_3)_2]$ (7)	0.760	0.780	0.791	0.777±0.030	0.810	0.810	0.879	0.833±0.047
$[MnCl_2(NO_3)(OAsPh_3)_2]$ (8)	0.623	0.725	0.694	0.681±0.009	0.630	0.780	0.763	0.724±0.023

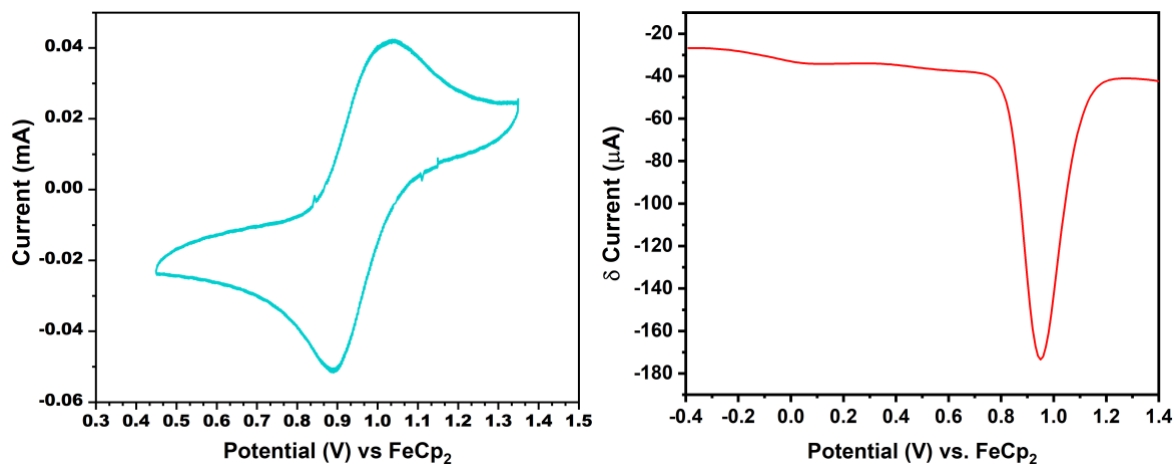


Figure S37: (Left) The cyclic voltammogram (200 mV/s, $i_{pc}/i_{pa} = 0.90$) and (right) differential pulse voltammogram of **2** in 0.5 M $[nBu_4N][PF_6]$ in DCM.

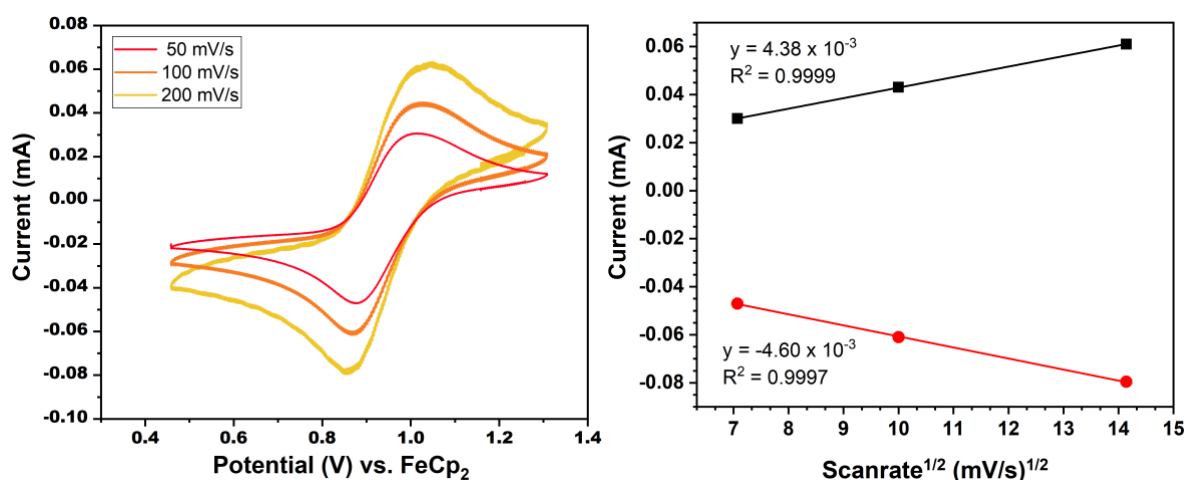


Figure S38: (Left) Cyclic voltammograms of **2** in 0.5 M $[nBu_4N][PF_6]$ in DCM at varying scan rates. (Right) Peak current vs. $(\text{scan rate})^{1/2}$ with linear fit.

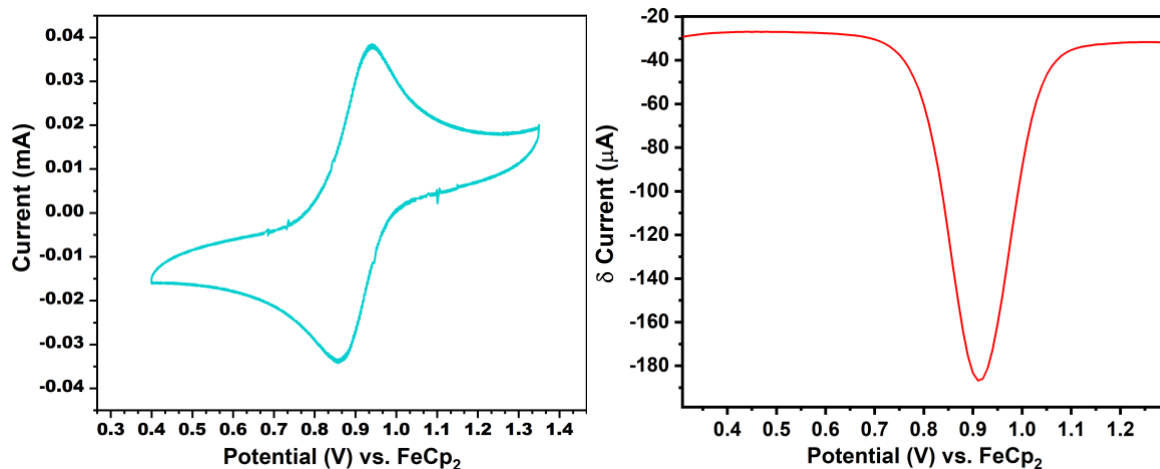


Figure S39: (Left) The cyclic voltammogram (200 mV/s, $i_{pc}/i_{pa} = 0.95$) and (right) differential pulse voltammogram of **4** in 0.5 M $[nBu_4N][PF_6]$ in DCM.

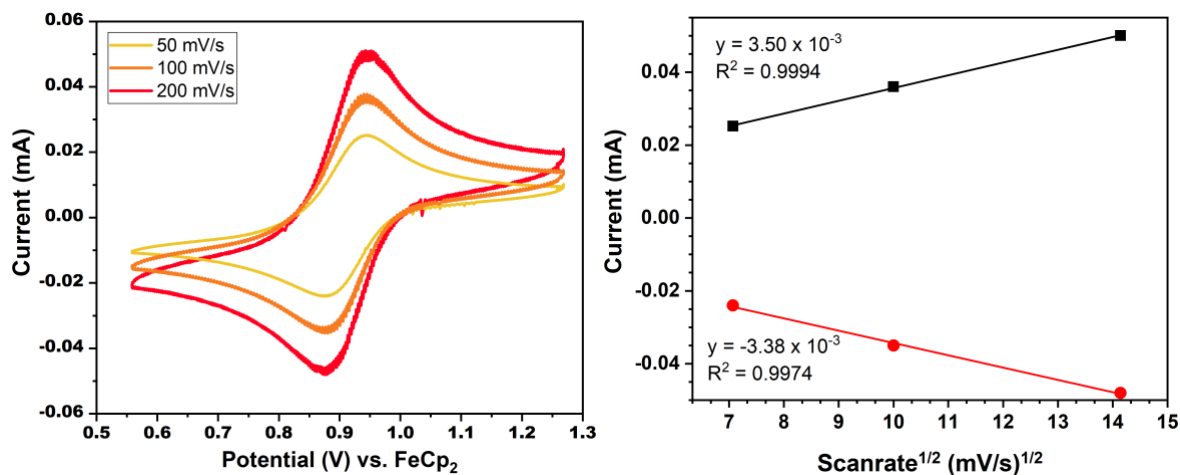


Figure S40: (Left) Cyclic voltammograms of **4** in 0.5 M [nBu₄N][PF₆] in DCM at varying scan rates. (Right) Peak current vs. (scan rate)^{1/2} with linear fit.

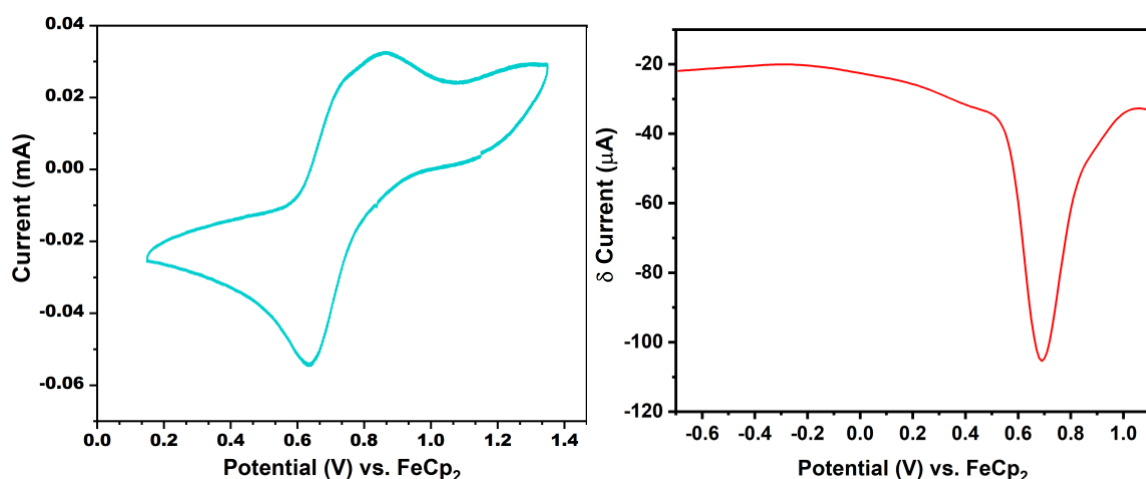


Figure S41: (Left) The cyclic voltammogram (200 mV/s, $i_{pc}/i_{pa} = 0.94$) and (right) differential pulse voltammogram of **6** in 0.5 M [nBu₄N][PF₆] in DCM.

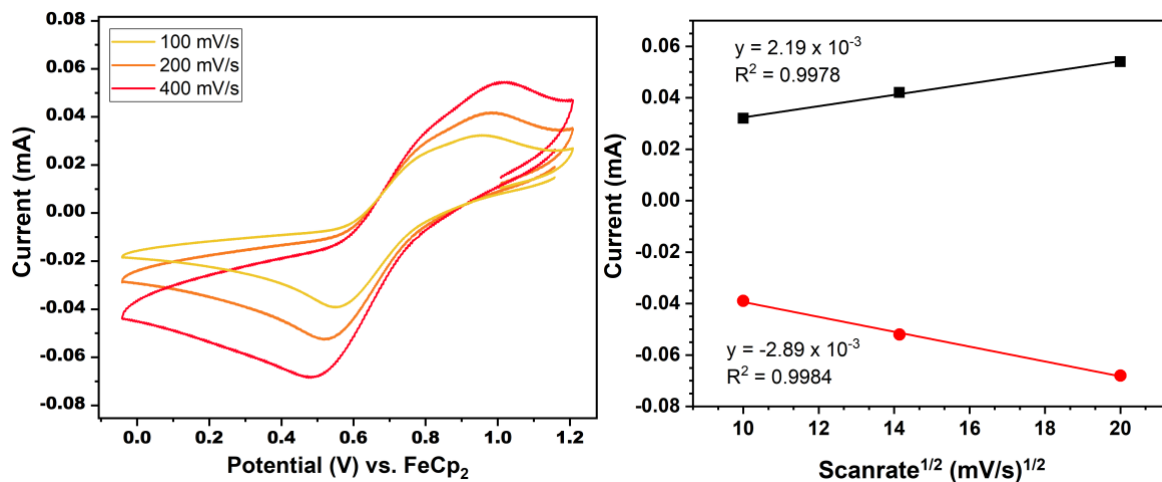


Figure S42: (Left) Cyclic voltammograms of **6** in 0.5 M [nBu₄N][PF₆] in DCM at varying scan rates. (Right) Peak current vs. (scan rate)^{1/2} with linear fit.

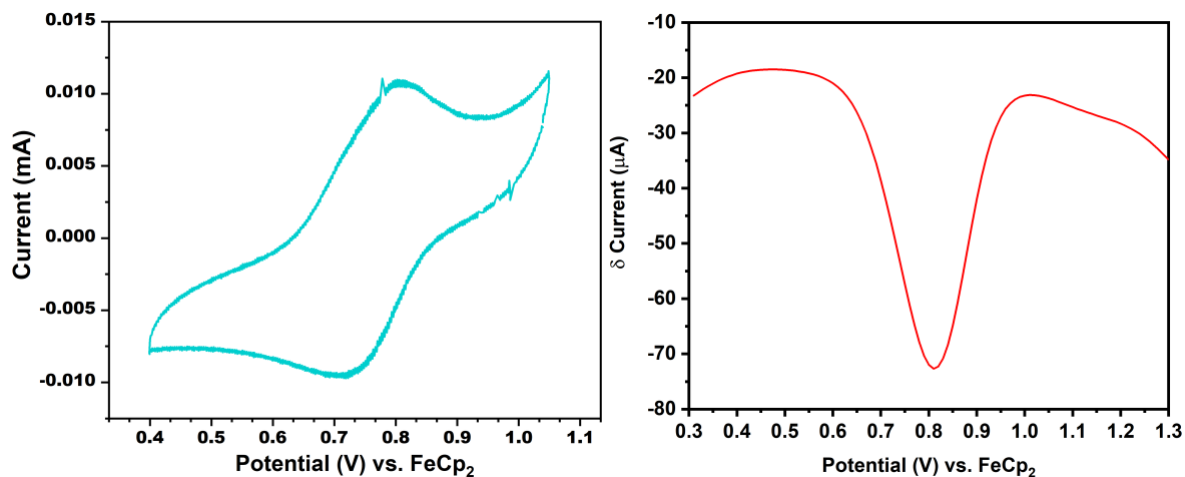


Figure S43: (Left) The cyclic voltammogram (200 mV/s, $i_{pc}/i_{pa} = 1.0$) and (right) differential pulse voltammogram of **7** in 0.5 M $[nBu_4N][PF_6]$ in DCM.

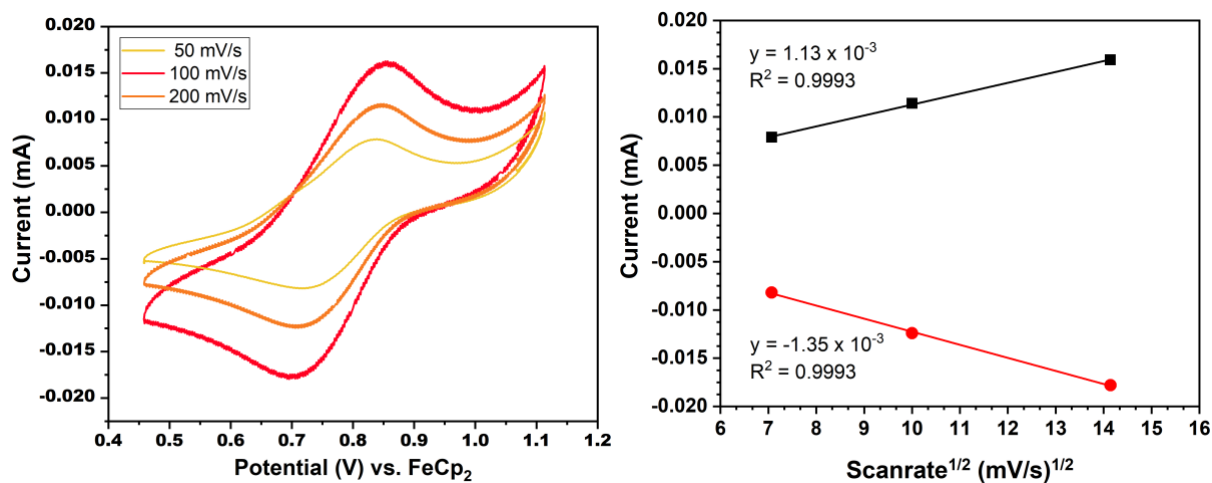


Figure S44: (Left) Cyclic voltammograms of **7** in 0.5 M $[nBu_4N][PF_6]$ in DCM at varying scan rates. (Right) Peak current vs. (scan rate)^{1/2} with linear fit.

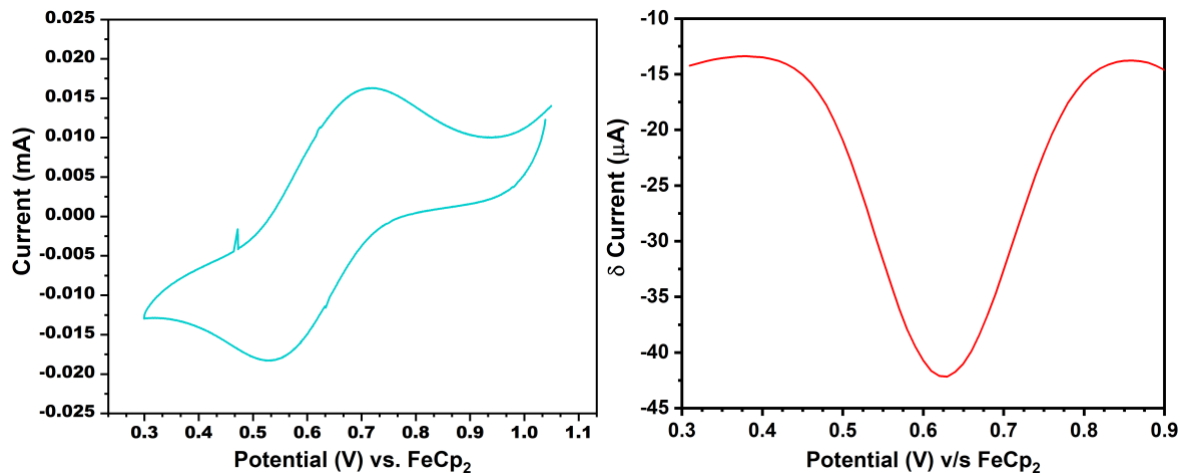


Figure S45: (Left) The cyclic voltammogram (200 mV/s, $i_{pc}/i_{pa} = 0.89$) and (right) differential pulse voltammogram of **8** in 0.5 M $[nBu_4N][PF_6]$ in DCM.

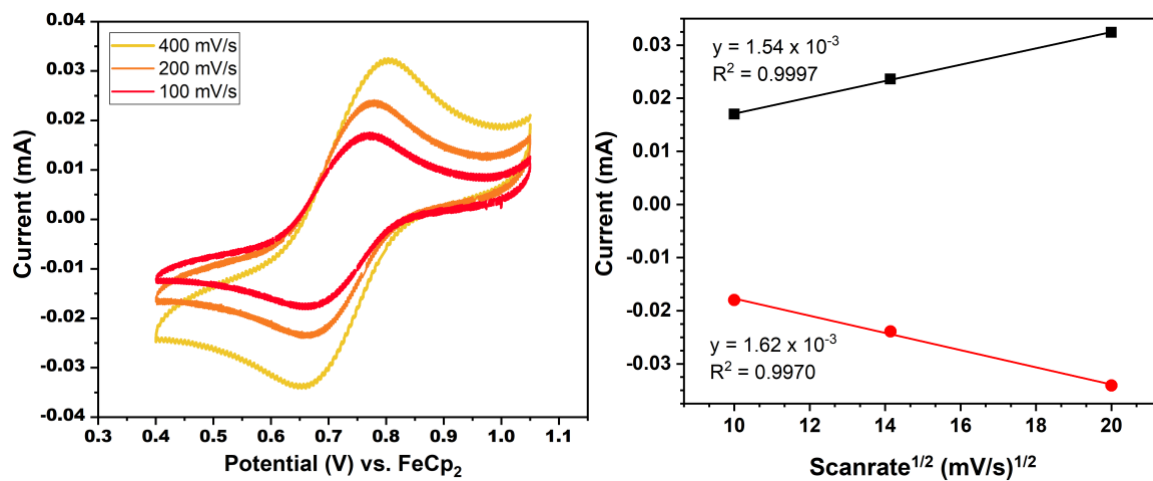


Figure S46: (Left) Cyclic voltammograms of **8** in 0.5 M [nBu₄N][PF₆] in DCM at varying scan rates. (Right) Peak current vs. (scan rate)^{1/2} with linear fit.

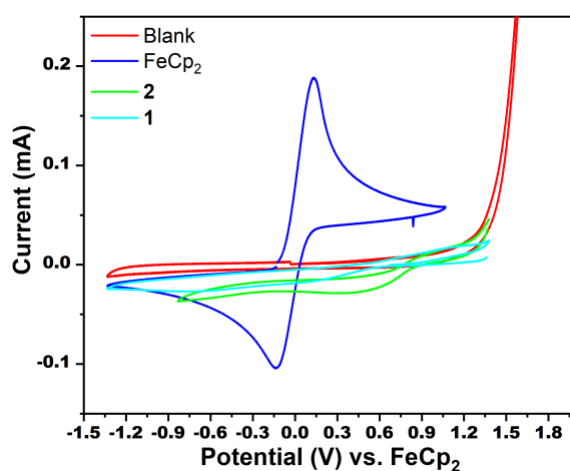


Figure S 47: Cyclic voltammograms of 6 mM solutions **1** and **2** in 0.5 M TBAPF₆ in THF compared to ferrocene. Complexes **1** and **2** are soluble in THF but decompose and may explain the lack of features. For example, the 6 mM solutions used to obtain these CVs decomposed in 3 to 4 hours.

Single-electron oxidation reactions

Oxidation of ferrocene by **2**

30 mM stock solutions of ferrocene and **2** in DCM were prepared separately. Into a quartz cuvette with a stir bar, ferrocene (15 mmol, 1.0 eq., 0.500 mL from stock solution of ferrocene) was added and volume adjusted to 2.9 mL. **2** (3.0 mmol, 0.2 eq., 0.100 mL from stock solution of **2**) was added to the solution and stirred at room temperature for 5 mins before a UV-vis spectrum was recorded. The procedure was repeated for 0 to 1.6 equivalents of **2**.

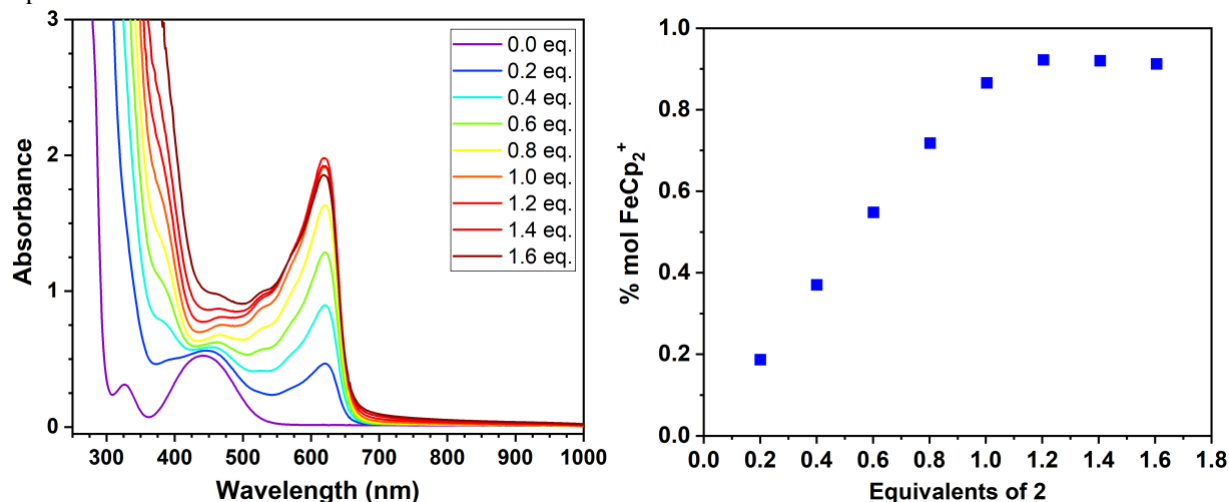


Figure S48: (Left) UV-vis spectra of reaction mixture in DCM after addition of varying equivalents of **2** and (right) corresponding plot for mole percentage of ferrocenium formed in the reaction mixture.

Table S3: Molar absorbance coefficients for reactants and products in DCM

Entry	Compound	λ_{\max} (nm)	ϵ (M ⁻¹ cm ⁻¹)
1	FeCp ₂	437	96
2	[FeCp ₂] ⁺	620	501

Oxidation of [Fe(bipy)₃](PF₆)₂ by **2**

10 mM stock solutions of [Fe(bipy)₃](PF₆)₂ and **2** in MeCN were prepared separately. Into a quartz cuvette with a stir bar, [Fe(bipy)₃](PF₆)₂ (8.0 mmol, 1.0 eq., 0.800 mL from stock solution of [Fe(bipy)₃](PF₆)₂) was added and volume adjusted to 4.0 mL. **2** (1.6 mmol, 0.2 eq., 0.020 mL from stock solution of **2**) was added to the solution and stirred at room temperature for 5 mins before a UV-vis spectrum was recorded. The procedure was repeated for 0 to 1.6 equivalents of **2**.

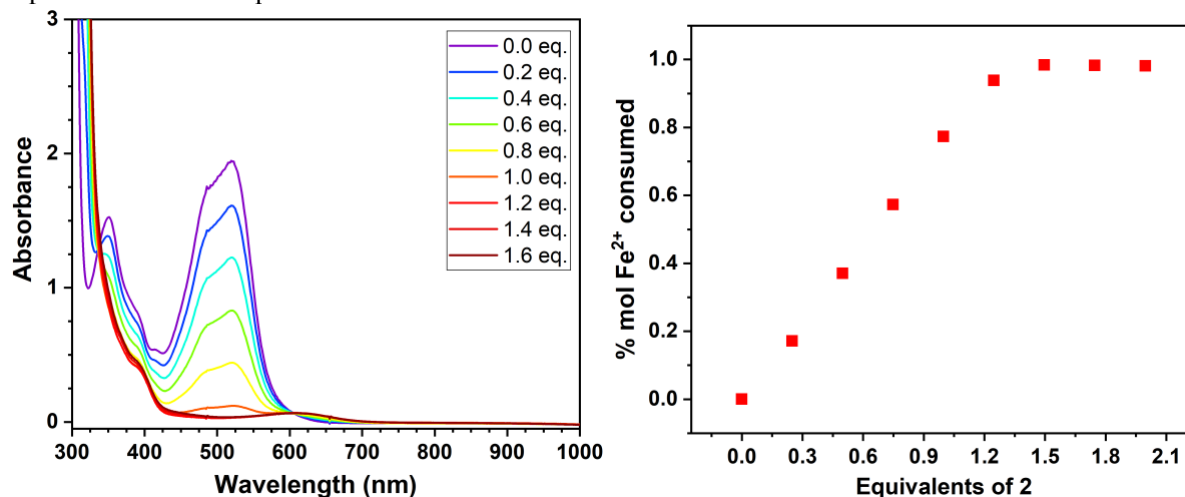


Figure S49: (Left) UV-vis spectra of reaction mixture in MeCN after addition of varying equivalents of **2** and (right) corresponding plot for mole percentage of [Fe(bipy)₃](PF₆)₂ consumed in the reaction mixture.

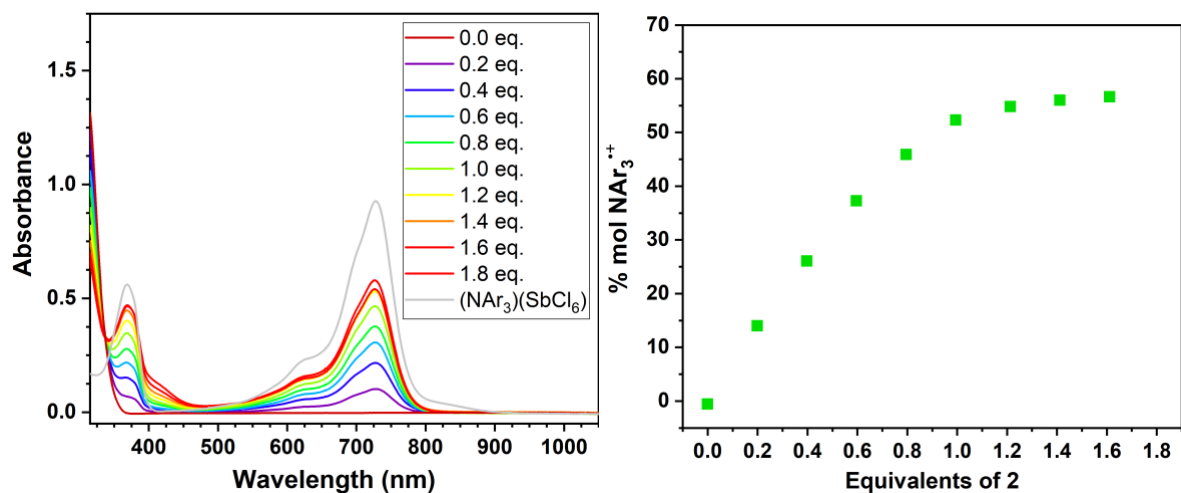
Table S4: Molar absorbance coefficients for reactants and products in MeCN

Entry	Compound	λ_{\max} (nm)	ϵ ($M^{-1}cm^{-1}$)
1	[Fe(bipy) ₃] ²⁺ (ref 9)	520	8240
2	[Fe(bipy) ₃] ³⁺ (ref 9)	609	261

Oxidation of tris(4-bromophenyl)amine by 2

1mM stock solutions of tris(4-bromophenyl)amine (NAr₃) and **2** in DCM were prepared separately. Into a quartz cuvette with a stir bar, NAr₃ (0.1 mmol, 1.0 eq., 0.100 mL from stock solution of NAr₃) was added and volume adjusted to 2.5 mL. **2** (0.02 mmol, 0.2 eq., 0.020 mL from stock solution of **2**) was added to the solution and stirred at room temperature for 5 mins before a UV-vis spectrum was recorded. The procedure was repeated for 0 to 1.8 equivalents of **2**.

Note: (NAr₃)(NO₃) was found to be unstable under experimental conditions, resulting in ~60% total conversion in multiple attempts. The epsilon for [NAr₃]^{•+} was determined from (NAr₃)(SbCl₆) purchase from Millipore Sigma.

**Figure S50:** (Left) UV-vis spectra of reaction mixture in DCM after addition of varying equivalents of **2** compared to authentic tris(4-bromophenyl)ammoniumyl hexachloroantimonate and (right) corresponding plot for mole percentage of tris(4-bromophenyl)ammoniumyl radical cation formed in the reaction mixture.**Table S5:** Molar absorbance coefficients for reactants and products in DCM

Entry	Compound	λ_{\max} (nm)	ϵ ($M^{-1}cm^{-1}$)
1	NAr ₃	--	--
2	(NAr ₃)(SbCl ₆)	725	26000

General procedure for solvent screen for HMB nitroxylation

To a 20 mL scintillation vial equipped with a stir bar, **2** or **4** (100-120 mg, 2.2 eq.) and 3 mL solvent was added; at this point, any additives (e.g., Et₃N) were also added. Under vigorous stirring, hexamethylbenzene (10 mg, 0.062 mmol, 1.0 eq.) was added to the reaction mixture and left to stir at room temperature until the deep color of the reaction mixture no longer remains. At the end of the reaction, all volatiles were removed under vacuum, and then reaction mixture was flushed through basic alumina plug using ~6 mL DCM. 10 mg 2-nitro benzaldehyde was added as internal standard and DCM was removed to get a pale-yellow residue. A small portion of the residue was dissolved in CDCl₃ to prepare NMR sample. ¹H-NMR spectrum was collected at room temperature, 32 scans with a relaxation delay of 1 second, and the products were quantified.

Table S6: Solvent screen for nitroxylation of hexamethylbenzene:

Entry	Conditions	Time	Percentage yield		Average yield (%)
			Run 1	Run 2	
1	DCM, 2.2 equiv. 2 , r.t.	5 m	99	98	98
2	DCM, 1.0 equiv. 2 , r.t.	<5 m	49	51	50
3	MeCN, 2.2 equiv. 2 , r.t.	15 m	96	94	95
4	THF, 2.2 equiv. 2 , r.t.	45 m	98	97	98
5	Fluorobenzene, 2.2 equiv. 2 , r.t.	45 m	69	69	69
6	Benzene, 2.2 equiv. 2 , r.t.	2.5 h	66	64	65
7	Benzene, 2.2 equiv. 2 , 1.5 equiv. Na ₂ CO ₃ , r.t.	2.5 h	64	--	64
8	Benzene, 2.2 equiv. 2 , 1.2 equiv. Et ₃ N, r.t.	2.5 h	8	--	8
9	Toluene, 2.2 equiv. 2 , r.t.	2.5 h	51	52	52
10	Pentane, 2.2 equiv. 2 , r.t.	20 h	44	57	51
11	DCM, 2.2 equiv. 4 , r.t.	24 h	60	55	58
Batch controls					
11	DCM, 2.2 equiv. 2 (crude), r.t.	5m	86	77	82
12	DCM, 2.2 equiv. 2 (crystallized outside glovebox), r.t.	5m	94	97	96

General procedure for nitroxylation reactions

Isolated yields: To a 20 mL scintillation vial equipped with a stir bar, **2** (150-250 mg, 2.2 eq.) was added and dissolved in 3-6 mL DCM. Once fully dissolved, substrate (1.0 eq.) was added and the reaction mixture was stirred at room temperature until the red-brown color of the reaction mixture no longer remains. Work-up began with addition of few drops of triethylamine to quench unreacted **2**. The reaction mixture was reduced to 0.5 mL with a rotary evaporator and loaded onto a basic alumina column. Product was eluted with 5-15% EtOAc/Hexanes.

NMR yields: Same procedure as above was followed. The quenched reaction mixture was flushed through a short basic alumina plug using ~6 mL DCM and 2-nitro benzaldehyde (~10 mg) was added to the combined DCM elute as internal standard. The DCM was removed to get a pale-yellow residue. A small portion of the residue was dissolved in CDCl₃ to prepare NMR sample. ¹H-NMR spectrum was collected at room temperature, 32 scans with a relaxation delay of 1 second, and the products were quantified.

2,3,4,5,6-pentamethylbenzyl nitrate: Following the general procedure for nitroxylation reactions: hexamethylbenzene (16.0 mg, 0.0986 mmol), for 5 minutes, to give 17.3 mg (86%) of 2,3,4,5,6-pentamethylbenzyl nitrate as a white solid. ¹H-NMR: (400MHz, CDCl₃) δ ppm 5.63 (s, 2 H), 2.31 (s, 3 H), 2.26 (s, 3 H), 2.24 (s, 3 H). ¹³C-NMR (101 MHz, CDCl₃) δ ppm 137.40, 135.60, 133.32, 124.94, 71.60, 17.37, 16.89, 16.63. ATR-FTIR (cm⁻¹): 2992, 2920, 2891, 1621 (ONO₂), 1608, 1557, 1491, 1450, 1371, 1291, 1276 (ONO₂), 960. Spectroscopic data matched literature values.¹⁰

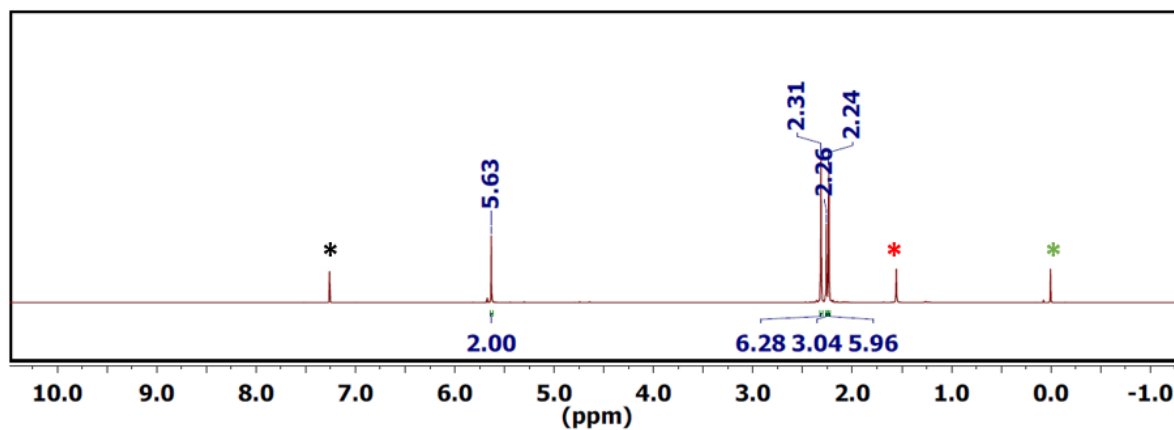


Figure S51: ^1H -NMR spectrum of 2,3,4,5,6-pentamethylbenzyl nitrate in CDCl_3 (*). * and * denote water and TMS respectively.

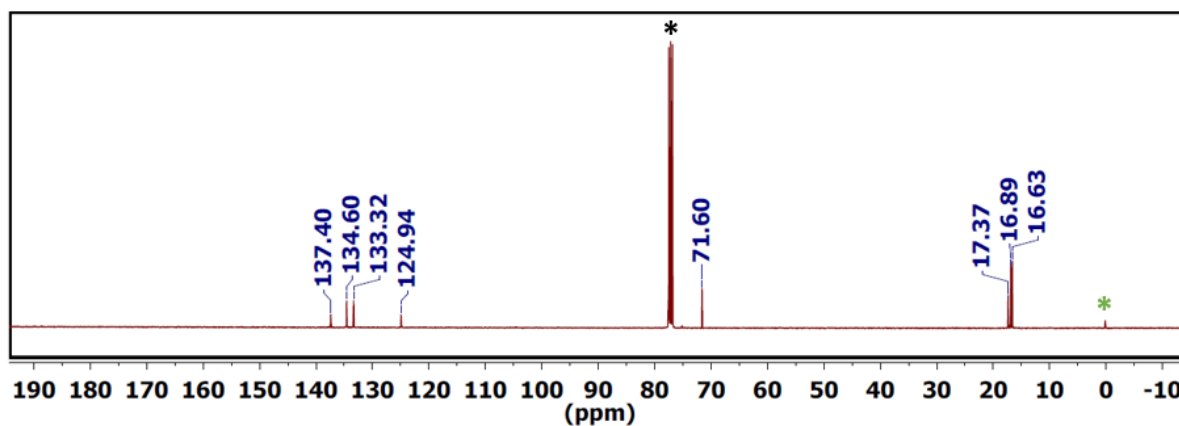


Figure S52: ^{13}C -NMR spectrum of 2,3,4,5,6-pentamethylbenzyl nitrate in CDCl_3 (*). * denotes TMS.

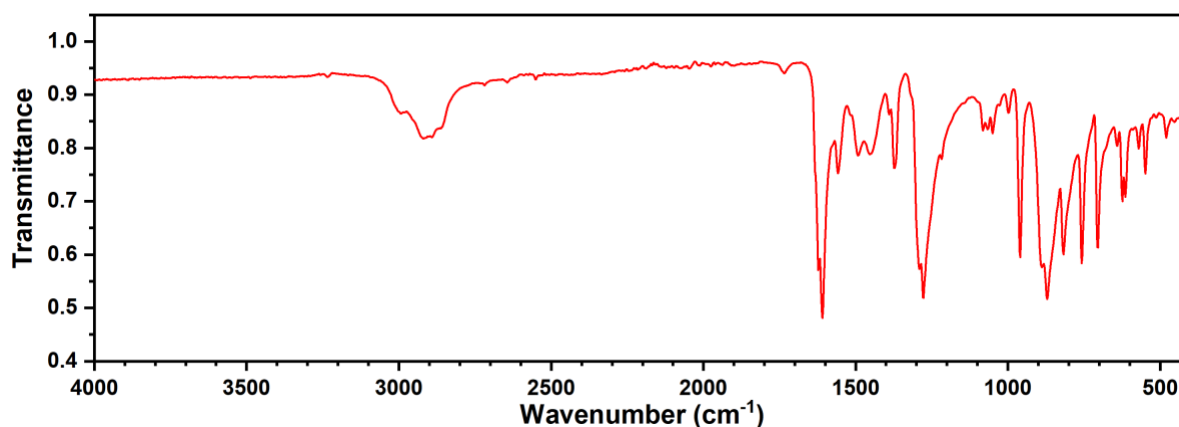


Figure S53: ATR-FTIR spectrum of 2,3,4,5,6-pentamethylbenzyl nitrate.

4-((tert-butyl)diphenylsilyloxy)benzyl nitrate: Following the general procedure for nitroxylation reactions: *tert*-butyldiphenyl(*p*-tolyl)oxy)silane (15.0 mg, 0.142 mmol), for 2.5 hours, to give 15.5 mg (89%) of 4-((*tert*-butyldiphenylsilyloxy)benzyl nitrate as a colorless oil. ^1H -NMR: (400MHz, CDCl_3) δ ppm 7.74 – 7.66 (m, 4H), 7.50 – 7.32 (m, 6H), 7.13 (d, J = 8.4 Hz, 2H), 6.77 (dd, J = 8.5, 1.6 Hz, 2H), 5.29 (s, 2H), 1.11 (s, 9H). ^{13}C -NMR (101 MHz, CDCl_3) δ ppm 156.90, 135.59, 132.61, 131.02, 130.18, 128.00, 124.46, 120.17, 75.08, 26.59, 19.59. ATR-FTIR (cm^{-1}): 3073, 3050, 2957, 2931, 2894, 2859, 1627 (ONO_2), 1608, 1512, 1473, 1427, 1390, 1361, 1256 (ONO_2), 1172, 1106, 908.

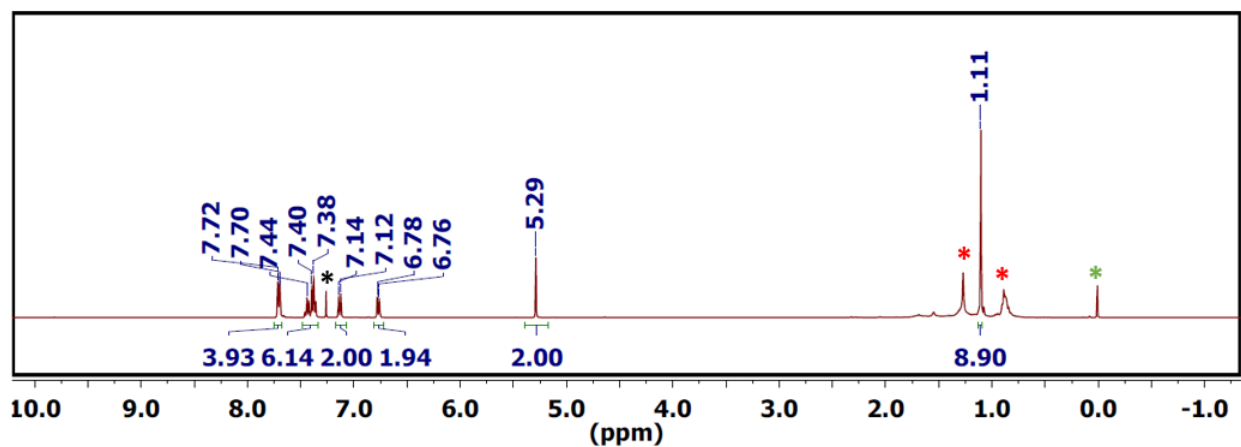


Figure S54: ^1H -NMR spectrum of 4-((*tert*-butyldiphenylsilyl)oxy)benzyl nitrate in CDCl_3 (*). * and * denote hexanes and TMS respectively.

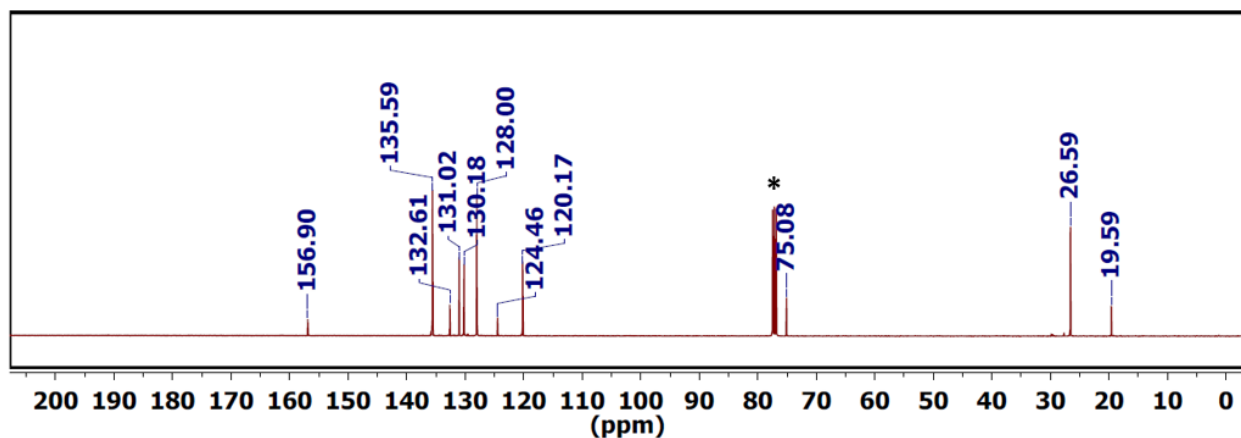


Figure S55: ^{13}C -NMR spectrum of 4-((*tert*-butyldiphenylsilyl)oxy)benzyl nitrate in CDCl_3 (*).

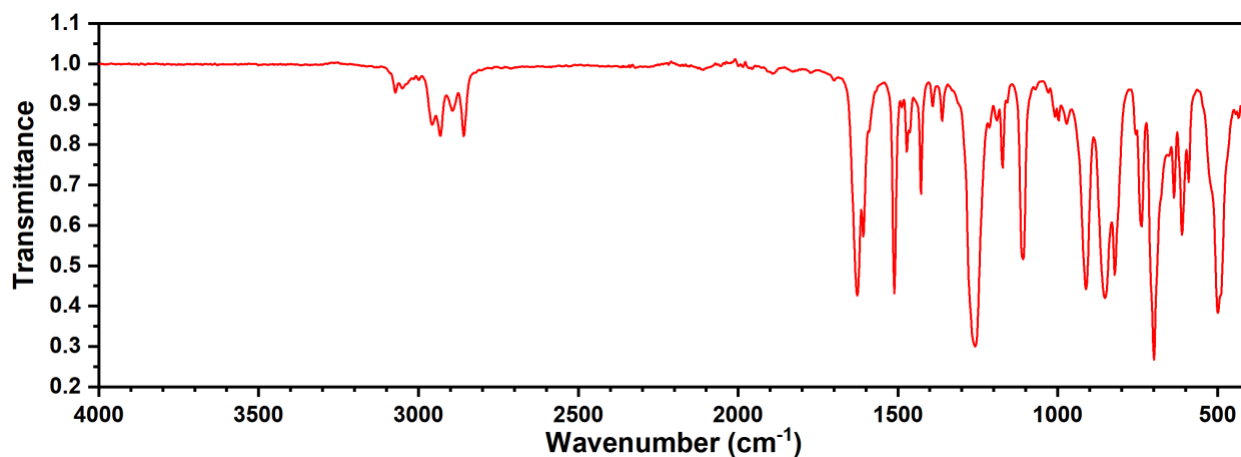


Figure S56: ATR-FTIR spectrum of 4-((*tert*-butyldiphenylsilyl)oxy)benzyl nitrate.

3,5-dimethylbenzyl nitrate: Following the general procedure for nitroxylation reactions: mesitylene (10.0 μL , 0.0719 mmol), for 24 hours, to give 3,5-dimethylbenzyl nitrate in 72% yield by ^1H -NMR: (400MHz, CDCl_3) δ ppm 6.09 (s, 3 H), 5.36 (s, 2 H), 2.33-2.28 (m, 6 H). Spectroscopic data matched literature values.¹¹

References

1. Eppley, H. J.; Christou, G., *Inorg. Syn.* **2002**, *33*, 61
2. Liu, H.-K.; Lei, Y.-F.; Tian, P.-J.; Wang, H.; Zhao, X.; Li, Z.-T.; et al. [Fe(bpy)₃]²⁺-based porous organic polymers with boosted photocatalytic activity for recyclable organic transformations. *J. Mater. Chem. A* **2021**, *9*, 6361.
3. Saju, A.; Griffiths, J. R.; MacMillan, S. N.; Lacy, D. C. Synthesis of a Bench-Stable Manganese(III) Chloride Compound: Coordination Chemistry and Alkene Dichlorination. *J. Am. Chem. Soc.* **2022**, *144*, 16761.
4. Wang, C.; Hong, H.; Chen, M.; Ding, Z.; Rui, Y.; Qi, J.; et al. A Cationic Micelle as In Vivo Catalyst for Tumor-Localized Cleavage Chemistry. *Angew. Chem. Int. Ed.* **2021**, *60*, 19750.
5. CrysAlisPro; Rigaku OD, The Woodlands, TX, 2015.
6. Sheldrick, G. M., SHELXT – Integrated Space-Group and Crystal-Structure Determination. *Acta Cryst.* **2015**, *A71*, 3.
7. Sheldrick, G.M. A Short History of SHELX. *Acta Cryst.* **2008**, *A64*, 112.
8. Müller, P. Practical Suggestions for Better Crystal Structures. *Crystallogr. Rev.* **2009**, *15*, 57.
9. Wong, C. L.; Kochi, J. K. Electron transfer with organometals. Steric effects as probes for outer-sphere and inner-sphere oxidations of homoleptic alkylmetals with iron(III) and iridate(IV) complexes. *J. Am. Chem. Soc.* **1979**, *101*, 5593.
10. Masnovi, J. M.; Sankararaman, S.; Kochi, J. K. Direct Observation of the Kinetic Acidities of Transient Aromatic Cation Radicals. The Mechanism of Electrophilic Side-Chain Nitration of the Methylbenzenes. *J. Am. Chem. Soc.* **1989**, *111*, 2263.
11. Baciocchi, E.; Rol, C.; Mandolini, L. Mechanism of oxidation of alkylaromatic compounds by metal ions. 3. A product study of the reaction of some polymethylbenzenes with cerium ammonium nitrate in acetic acid. *The Journal of Organic Chemistry* **1977**, *42*, 3682.